

UNIVERSITY OF OKLAHOMA
GRADUATE COLLEGE

ROCK PROPERTIES DERIVED FROM ANALYSIS OF EARTH TIDE STRAIN
OBSERVED IN CONTINUOUS PRESSURE MONITORING OF THE ARBUCKLE
GROUP OF OKLAHOMA

A THESIS
SUBMITTED TO THE GRADUATE FACULTY
in partial fulfillment of the requirements for the
Degree of
MASTER OF SCIENCE

By
PAULA JULIANA PERILLA CASTILLO
Norman, Oklahoma
2017

ROCK PROPERTIES DERIVED FROM ANALYSIS OF EARTH TIDE STRAIN
OBSERVED IN CONTINUOUS PRESSURE MONITORING OF THE ARBUCKLE
GROUP OF OKLAHOMA

A THESIS APPROVED FOR THE
CONOCOPHILLIPS SCHOOL OF GEOLOGY AND GEOPHYSICS

BY

Dr. Kyle E. Murray, Co-Chair

Dr. Douglas R. Elmore, Co-Chair

Dr. Norimitsu Nakata

© Copyright by PAULA JULIANA PERILLA CASTILLO 2017
All Rights Reserved.

To God, who continues to give me the strength to pursue my dreams.

To my mother and all the Perilla Castillo family.

Acknowledgements

I would like to thank specially my advisor, Dr. Kyle E. Murray, for his constant guidance and support through all this process and the great opportunity he gave me to come to Oklahoma. I would also like to thank the Oklahoma Geological Survey and the Oklahoma Independent Petroleum Association for funding this research. To the Oklahoma Geological Survey for funding me and giving me the opportunity to continue my studies in the University of Oklahoma. My research would have never been achievable without the help of Jordan Williams in guidance and trial-error discussions and Curtis Smith and Ella Walker in instrumenting the wells and collecting the data. Finally, I would like to thank my mother, my family, and my friends, their encouragement, prayers, and words of support have helped me through this part of my life.

Table of Contents

| | |
|---|----|
| Acknowledgements | iv |
| Abstract..... | xi |
| Chapter 1: Introduction..... | 1 |
| 1.1 Background and Previous Studies | 2 |
| 1.2 Geologic and Hydrogeologic Setting | 5 |
| 1.3 Study Area | 9 |
| 1.4 Research Objectives | 11 |
| Chapter 2: Methodology..... | 12 |
| 2.1 Pressure Monitoring Instrumentation | 12 |
| 2.2 Normalization of Data | 13 |
| 2.3 Baseline Trends | 13 |
| 2.4 Tidal Signal | 13 |
| 2.5 Computation of properties | 15 |
| 2.5.1 Specific Storage | 15 |
| 2.5.2 Storage Coefficient | 18 |
| 2.5.3 Transmissivity | 19 |
| 2.5.4 Matrix Compressibility..... | 21 |
| 2.5.5 Hydraulic Conductivity | 22 |
| 2.5.6 Intrinsic Permeability | 23 |
| 2.5.7 Hydraulic Diffusivity..... | 23 |
| 2.6 Barometric Efficiency..... | 23 |
| 2.7 Reservoir Porosity | 26 |

| | |
|--|----|
| Chapter 3: Present Study | 27 |
| 3.1 Introduction | 27 |
| 3.2 Objectives | 28 |
| 3.3 Materials and Methods | 29 |
| 3.3.1 Estimation of Specific Storage | 31 |
| 3.3.2 Estimation of Storage Coefficient | 33 |
| 3.3.3 Estimation of Transmissivity | 33 |
| 3.3.4 Estimation of Matrix Compressibility | 34 |
| 3.3.5 Estimation of Barometric Efficiency | 34 |
| 3.3.6 Estimation of Porosity | 35 |
| 3.3.7 Hydraulic Conductivity | 36 |
| 3.3.8 Intrinsic Permeability | 36 |
| 3.3.9 Hydraulic Diffusivity | 36 |
| 3.4 Results and Discussion | 37 |
| 3.4.1 Specific Storage | 38 |
| 3.4.2 Storage Coefficient | 39 |
| 3.4.3 Transmissivity | 40 |
| 3.4.4 Matrix Compressibility | 41 |
| 3.4.5 Barometric Efficiency | 42 |
| 3.4.6 Reservoir Porosity | 43 |
| 3.4.7 Hydraulic Conductivity | 44 |
| 3.4.8 Intrinsic Permeability | 45 |
| 3.4.9 Hydraulic Diffusivity | 46 |

| | |
|---|----|
| Chapter 4: Conclusions..... | 47 |
| References | 49 |
| Appendix A: Monitoring Wells Observed Solid Earth Tides | 52 |
| A-1 Well Alfalfa 03..... | 53 |
| A-2 Well Alfalfa 04..... | 54 |
| A-3 Well Grant 06 | 55 |
| A-4 Well Lincoln 10..... | 56 |
| A-5 Well Pawnee 11..... | 57 |
| A-6 Well Logan 12..... | 58 |
| Appendix B: Frequency Spectrum For Monitoring Wells And Theoretical Solid Earth | |
| Tides | 59 |
| B-1 Well Alfalfa 03 | 60 |
| B-2 Well Alfalfa 04..... | 61 |
| B-3 Well Grant 06 | 62 |
| B-4 Well Lincoln 10..... | 63 |
| B-5 Well Pawnee 11 | 64 |
| B-6 Well Logan 12 | 65 |

List of Tables

| | |
|---|----|
| Table 1. Five main harmonic components of tides with values compiled from Merritt (2004). | 14 |
| Table 2. Parameters for diurnal and semidiurnal equilibrium tides, from Munk and MacDonald (1960) and Doodson and Warburg (1941)..... | 17 |
| Table 3. Amplitudes and lags in time for the tidal components O_1 and M_2 in the water level record for the studied wells..... | 38 |
| Table 4. Summary of values obtained for each property computed from solid earth tides time series analyses. | 48 |

List of Figures

| | |
|---|----|
| Figure 1. Rock types of Late Cambrian to Early Ordovician age (Modified from Johnson (2008)). | 7 |
| Figure 2. Cross section from the Anadarko Shelf in northwestern Oklahoma (Modified from Johnson (2008)). | 9 |
| Figure 3. Monitoring wells in study area for tidal strain analysis. | 10 |
| Figure 4. Ratio of amplitudes of the well water level and reservoir pressure head oscillations as a function of dimensionless transmissivity, from Merritt (2004). | 20 |
| Figure 5. Phase lag between the well water-level and reservoir pressure head oscillations as a function of dimensionless transmissivity, from Merritt (2004). | 21 |
| Figure 6. Amplitudes of M_2 and S_2 components in the theoretical tidal strain for well Alfalfa 03 to calculate $S_2:M_2$ ratio. | 25 |
| Figure 7. Time series for the well Alfalfa 03. Fig 7a. shows the water level fluctuations measurement. Fig 7b. shows the filtered data (FFT band pass filter cutoff frequency 1.5 cpd and band width 1 cpd). Fig 7c. shows the theoretical tide generating potential. | 30 |
| Figure 8. Spectrum of tidal components in filtered data from well Alfalfa 03. Each tidal component is identified. | 31 |
| Figure 9. Range of S_s computed values from solid earth tide analyses (present study) and comparison from previous studies. | 39 |
| Figure 10. Range of S computed values from solid earth tide analyses (present study) and comparison from previous studies. | 40 |
| Figure 11. Range of T computed values from solid earth tide analyses (present study) and comparison to previous studies. | 41 |

| | |
|---|----|
| Figure 12. Range of α computed values from solid earth tide analyses (present study) and comparison to textbook value. | 42 |
| Figure 13. Range of BE computed values from solid earth tide analyses (present study) and comparison from previous studies. | 43 |
| Figure 14. Range of η computed values from solid earth tide analyses (present study) and comparison from previous studies. | 44 |
| Figure 15. Range of K computed values from solid earth tide analyses (present study) and comparison to previous studies. | 45 |
| Figure 16. Range of k_i computed values from solid earth tide analyses (present study) and comparison from previous studies. | 45 |
| Figure 17. Range of D computed values from solid earth tide analyses (present study) and comparison from previous studies. | 46 |

Abstract

The Arbuckle Group is an important geologic unit in the state of Oklahoma because of its suitability as a saltwater disposal (SWD) zone. In 2014, the Arbuckle Group received about 68% of the total volumes of saltwater disposal in the state of Oklahoma. Numerous studies show that the rate of saltwater injection into the Arbuckle Group is related to the number and magnitude of earthquakes occurring in Oklahoma. Despite the importance of the Arbuckle Group as a SWD zone and its apparent relationship to induced seismicity, the hydraulic parameters of the Arbuckle Group have not been widely studied or were studied in association with the Simpson Group.

Since the mid-20th century, water level fluctuations as a response to earth tides have been used for obtaining aquifer properties of confined and unconfined aquifers. In confined aquifers, earth tides act as a cyclic stress causing water level fluctuations. Time-series analyses of the fluctuations can be used for estimating elastic properties of an aquifer and aquifer hydraulic properties such as specific storage, storage coefficient, transmissivity, porosity, matrix compressibility, hydraulic conductivity, and hydraulic diffusivity. Solid earth tide analysis is a useful tool for calculating rock properties in aquifers or reservoirs where it is not practical to conduct a pumping or a slug test. Confined reservoirs such as the Arbuckle Group respond to small strains and act as volume strain meters.

In 2016, a network of inactive Arbuckle SWD wells were instrumented so that pressure fluctuations could be monitored and analyzed. For this thesis research, fluid levels in six of the study wells were evaluated. Fluid levels responded to solid earth tide stresses so that 90-day time series could be analyzed and used to estimate hydraulic and

rock properties of the Arbuckle Group in the Anadarko Shelf and the Cherokee Platform geological provinces of Oklahoma. Hydraulic parameters derived from these analysis of these data include median values of $1.39 \text{ E-}06 \text{ m}^{-1}$ specific storage, $3.69 \text{ E-}04$ storage coefficient, $12.76 \text{ m}^2/\text{d}$ transmissivity, 24% porosity, $3.02 \text{ E-}07 \text{ psi}^{-1}$ matrix compressibility, $2.21 \text{ E-}07 \text{ m/s}$ hydraulic conductivity, 34.37 mD intrinsic permeability, and $0.69 \text{ m}^2/\text{s}$ hydraulic diffusivity. Values obtained for each of the properties computed in this study differ from the values used in previous studies that modeled the effects of saltwater disposal on subsurface fluid pressure and potential connections to seismicity. These improved values will allow for more realistic predictions of subsurface fluid behavior, pore pressure diffusion, and other geomechanical and seismological processes.

Chapter 1: Introduction

Since the mid-20th century, water level fluctuations as a response to earth tides have been used for obtaining aquifer properties of confined and unconfined aquifers (Cutillo and Bredehoeft, 2011). In confined aquifers, earth tides act as a cyclic stress causing water level fluctuations. Time-series analysis of the fluctuations can be used for estimating elastic properties of an aquifer and aquifer hydraulic properties such as specific storage, storage coefficient, transmissivity, porosity, matrix compressibility, permeability, hydraulic conductivity, and hydraulic diffusivity (Bernard and Delay, 2008; Cutillo and Bredehoeft, 2011; Mehnert et al., 1999).

The Arbuckle Group is a confined reservoir that underlies a large part of the state of Oklahoma and is comprised mainly by carbonates (Ragland and Donovan, 1991). Downhole pressure was monitored for several inactive wells in Alfalfa, Grant, Lincoln, Logan, and Pawnee Counties as early as August 2016. The open intervals of the wells are in the Arbuckle Group and, in most cases, have no observed effects or stresses from production or injection; therefore, water level fluctuations are largely due to solid earth tides.

The objective of this study was to analyze the naturally-induced stress of earth tides that are present in the time series to obtain the elastic and hydraulic properties of the Arbuckle Group in areas of the Anadarko Shelf and the Cherokee Platform. Water level responses and theoretical solid earth tides are used to analyze the phase lag between the water level fluctuations and the theoretical tides for the aquifer parameters, and the barometric efficiency to estimate porosity (Cutillo and Bredehoeft, 2011; Rahi, 2010).

1.1 Background and Previous Studies

The Earth's surface can be considered a "free surface" in the sense that the vertical direction is the principal direction for strain tensors. Natural stresses, such as tidal strain, atmospheric pressure load, and oceanic tides are able to move the surface of the earth up or down (Rahi, 2010). Earth and ocean tides are products of lunar and solar tidal forces (Rahi, 2010). Earth tides stress inland aquifers and reservoirs, generating measurable fluctuations in water levels (Cuttillo and Bredehoeft, 2011; Rahi, 2010). Tidal strain occurs in the horizontal plain as a wave phenomenon twice a day, with amplitude of the horizontal component of 10^{-8} (Cuttillo and Bredehoeft, 2011).

The tidal gravitational potential can be described as a set of harmonic functions, with each tidal component having a distinct amplitude (A), frequency (f), and phase relation (Φ). There are five principal components of the tidal potential, which are the M_2 and N_2 semidiurnal lunar tides, the S_2 semidiurnal solar tide, the O_1 diurnal lunar tide, and the K_1 diurnal lunar-solar tide (Cuttillo and Bredehoeft, 2011).

Water level fluctuations as a response to tidal strain have been reported in the literature since 1880. Melchior (1956) performed harmonic analysis on a data set from one deep well and one hot spring. In 1960, Melchior expanded the harmonic analysis to previous data sets, including a data set from Theis from Carlsbad, New Mexico. He assumed the aquifer was a finite cavity, developed a mathematical formulation that relates displacement in water caused by a change in volume, and was able to calculate dilatation. With the relationship developed by Melchior, it was estimated that the semidiurnal component of the tide produces a dilatation with an amplitude of 2×10^{-8} , which corresponds to a water level fluctuation of about 0.4 cm (Bredehoeft, 1967).

Nonetheless, Melchior observed an amplitude of about 2 cm in his data set. Later on, the phase lag between the theoretical tides and the actual observations was used to develop a relationship to estimate aquifer properties.

Bredehoeft (1967) compiled data for water level fluctuations from the literature and the theory explaining the fluctuations. Bredehoeft (1967) described the response of a well to tidal strain for confined and unconfined aquifers, as well as the tidal deformation and relationship between stress and strain and gives formulas to obtain specific storage and porosity from tidal components.

Marsaud et al. (1993) used time series analysis to investigate the relationship between barometric efficiency, earth tides, and water level fluctuations in a confined aquifer to estimate porosity, storage coefficient, and aquifer thickness. In their study, they describe the influence of the atmospheric pressure load in changes in water levels and influence of earth tides. The authors analyze the validity of the theory in a karstic aquifer and how spectral analysis can be applied to obtain parameters. Marsaud et al. (1993) correlated the results obtained from the earth tides method with pumping test analysis and concluded that tidal strain analysis can improve aquifer parameter estimation.

Mehnert et al. (1999) estimated transmissivity from water level fluctuations of a sinusoidal forced well. Fluctuations as a response to earth tides and changes in atmospheric pressure were analyzed, assuming that atmospheric pressure varied in a sinusoidal fashion. Using type curves and estimation of the ratio of amplitudes of the fluctuations, Mehnert et al. (1999) presented a simpler model for calculation of transmissivity that allows for the estimation of transmissivity for limited time series

data with satisfactory estimations of transmissivity from 116 observations recorded over 3.5 minutes.

Maréchal et al. (2002) analyzed cyclic fluctuations in an unconfined crystalline rock aquifer using short-interval water level measurements with an automatic water level recorder. The authors analyzed earth tides and precipitation to determine the forces influencing the fluctuations in water levels. Spectral analyses carried out by Maréchal et al. (2002) concluded that the fluctuations observed in the well were a response to earth tides rather than effects from pumping in nearby wells or precipitation patterns. Tesserale waves of daily period and sectorial waves of semi-daily period were identified in the dataset. The analysis indicated low porosity for the aquifer, as could be expected for a crystalline rock aquifer.

Bernard and Delay (2008) used correlation and spectral analyses of time series to determine porosity and storage coefficient in a calcareous aquifer. In their study, time-series analysis was used to understand the relationship between barometric pressure changes, earth tides, and water level fluctuations. The relationships were used to estimate porosity, storage capacity, and barometric efficiency. Flow between fracture matrix drainage and karstic features was observed in thin confined layers of the aquifer. Despite the mixed conditions in the aquifer, the earth tides method was able to produce accurate estimates for the aquifer's parameters, compared to results obtained from pumping tests. The authors concluded that time series analysis can be used even for complex flow environments.

Rahi (2010) estimated aquifer parameters of the Arbuckle-Simpson Aquifer in south-central Oklahoma by analyzing water level fluctuations in nine wells. Applying

the methods of the previous studies, Rahi (2010) estimated specific storage values of 5.4×10^{-8} and 2.1×10^{-7} for wells tapping confined portions of the aquifer and wells tapping semi-confined portions, respectively. Porosity calculated for the Arbuckle-Simpson aquifer by the barometric efficiency method ranged from 15% to 45% in confined and semi-confined portions, respectively.

Cutillo and Bredehoeft (2011) analyzed another confined carbonate aquifer in California. The water level fluctuations used in their study were from a deep open well completed in a Paleozoic age confined aquifer. Using tidal strain analysis and a set of harmonic functions, the authors estimated amplitudes, frequency, and phase relation for the five principal components that comprise tidal potential. With the data set and the harmonic analysis, Cutillo and Bredehoeft (2011) estimated specific storage from the relationship between water level fluctuations and tidal dilatation and used barometric efficiency to estimate porosity. Finally, with areal tidal strain analysis they estimated specific storage and porosity to compare with the first series of results. Moreover, they could calculate Skempton's coefficient, transmissivity, and matrix compressibility.

1.2 Geologic and Hydrogeologic Setting

The Arbuckle Group is a geological unit of Cambrian to Early Ordovician age composed mainly of carbonates (Johnson, 1991). In Oklahoma, the Arbuckle Group is comprised of six formations including the West Spring Creek Formation (top), Kindblade, Cool Creek, McKenzie Hill, Signal Mountain, and the Fort Sill Formation (base) (Ragland and Donovan, 1991). The group underlies nearly the entire state of Oklahoma and outcrops in southwestern Oklahoma in the Slick Hills, in the Wichita

Uplift geological province, and in south-central Oklahoma in the Arbuckle Uplift geological province (Morgan and Murray, 2015).

The Arbuckle Group comprises the mid-southern part of what is known as the Great American Carbonate Bank (GACB) (Fritz et al., 2013). It is composed of cyclic carbonates dominated by intertidal and shallow subtidal facies (Fritz et al., 2013). The deposition of the Arbuckle Group began in the Late Cambrian, after the rifting and formation of the Oklahoma aulacogen (Christenson et al., 2011). During the Late Cambrian to Early Ordovician, shallow seas extended from what is known today as Northern Mexico to Canada, depositing carbonate sediments in an almost flat ramp (Figure 1) (Christenson et al., 2011; Johnson, 2008). The Arbuckle Group equivalent units in neighboring states include the El Paso Group in west Texas, the Ellenburger Group in central and north Texas, the Knox Group in the eastern United States, and the Beekmantown Group in the northeastern United States (Morgan and Murray, 2015).

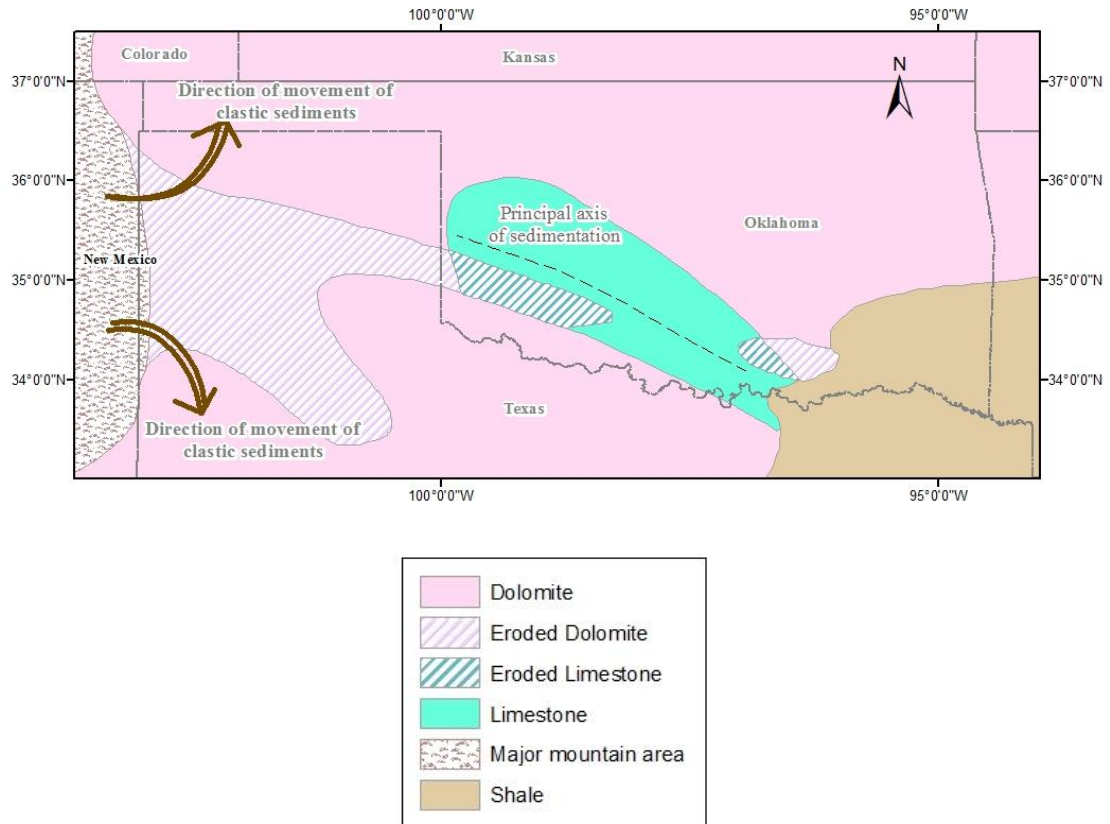


Figure 1. Rock types of Late Cambrian to Early Ordovician age (Modified from Johnson (2008)).

The thickness of the Arbuckle Group can range from approximately 1,000 ft to 2,000 ft in the Anadarko Shelf and Cherokee Platform to 7,000 ft in the Anadarko Basin, Ardmore Basin, and in the Arbuckle Uplift (Johnson, 1991, 2008). The top of the Arbuckle can be more than 30,000 ft below land surface in the Anadarko Basin or outcropping in other regions (Morgan and Murray, 2015).

The dolomites of the Arbuckle Group have been susceptible to dissolution during cycles of uplift and erosion, which created unconformities within the Arbuckle. Cycles of karstification and diagenetic alterations in the rocks, such as dolomitization, have also augmented the porosity and generated cavernous areas (Carr et al., 1986).

Hydraulic parameters of the Arbuckle Group have not been widely studied or were studied in association with the Simpson Group since both units comprise the Arbuckle-Simpson Aquifer in south-central Oklahoma (Christenson et al., 2009; Christenson et al., 2011). The Arbuckle Group can be characterized as a confined aquifer, underlying the Simpson Group. In the areas where the group is almost superficial or outcrops, the water contained within the unit is freshwater (Christenson et al., 2011). Freshwater from the group, in general, can be used for public supply, being suitable for all regulated uses (Christenson et al., 2009). In other parts of Oklahoma, the Arbuckle is deeper and more appropriately referred to as a reservoir, because it contains brine and petroleum rather than freshwater.

The Arbuckle Group has been commonly used as a saltwater disposal (SWD) zone in the areas where it is deep below the land surface. In 2014, the Arbuckle Group received about 68% of the total volumes of saltwater injected into the subsurface in Oklahoma (Murray, 2015). The Arbuckle has shown a capacity for receiving vast amounts of saltwater and residues from the oil and gas industry, with little or no injection pressure (Carrell, 2014). Despite the common use of the Arbuckle Group as a SWD zone, the regional variations in hydraulic properties and the pressure regime of the Arbuckle are poorly understood.

1.3 Study Area

The study area is located in northwestern and north central Oklahoma, in Alfalfa, Grant, Pawnee, Lincoln, and Logan Counties in the Anadarko Shelf and Cherokee Platform geological provinces of Oklahoma (Northcutt and Campbell, 1995). In the Anadarko Shelf, the rocks are lying in an almost flat configuration, with a very low inclination of the layers (Johnson, 2008) (Figure 2).

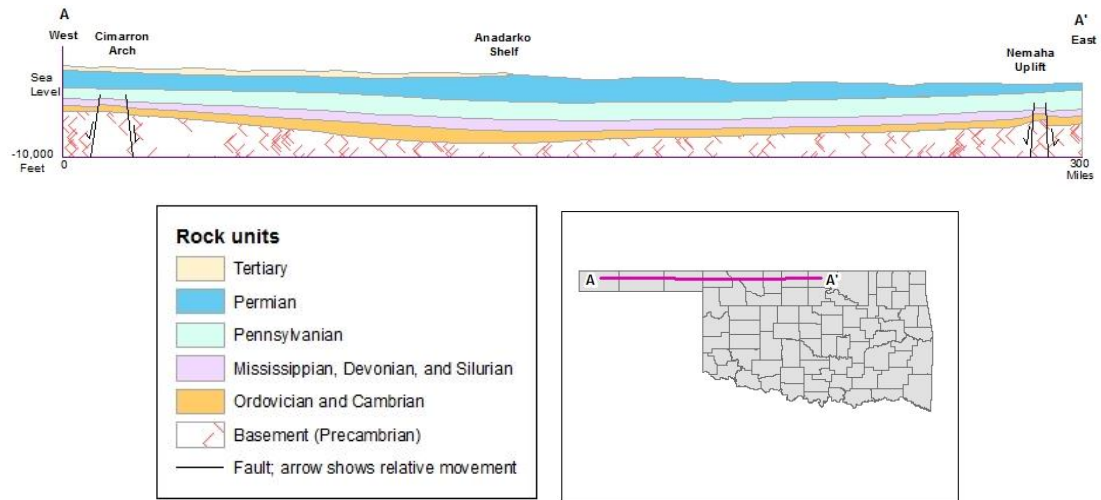


Figure 2. Cross section from the Anadarko Shelf in northwestern Oklahoma (Modified from Johnson (2008)).

In the study area, there are six inactive SWD wells that were instrumented with pressure transducers in August 2016. The wells have their open interval in the Arbuckle Group. Figure 3 presents the locations of the instrumented wells. Depth to water below the land surface ranged from 73 feet to 375 feet.

LOCATION OF MONITORING WELLS

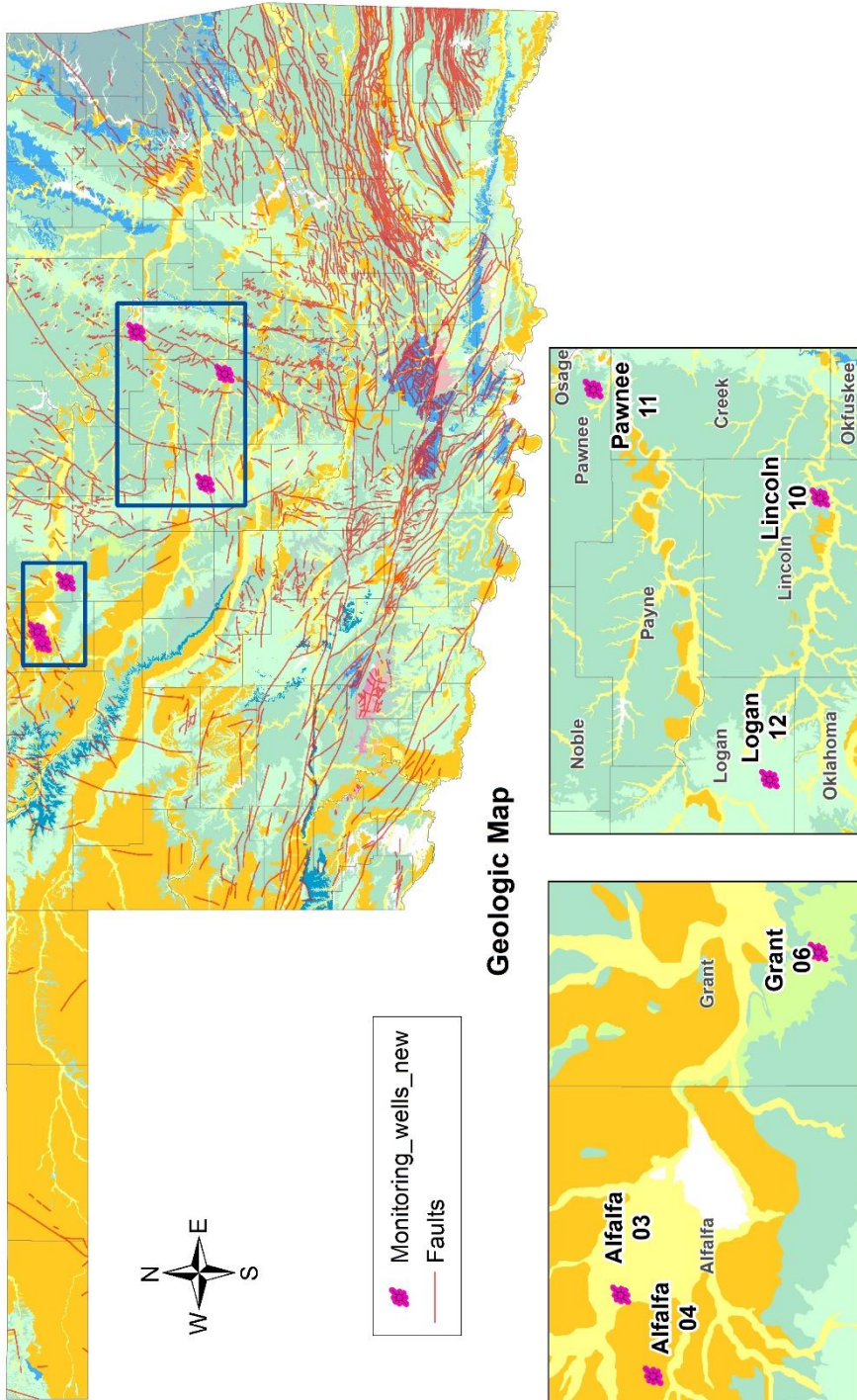


Figure 3. Monitoring wells in study area for tidal strain analysis.

1.4 Research Objectives

Water level fluctuation as a result of tidal strain was analyzed to estimate rock properties and parameters for the Arbuckle Group in northwestern and north-central Oklahoma. Spectral analysis of time series and application of fast Fourier transforms was used to calculate specific storage, storage coefficient, transmissivity, porosity, matrix compressibility, hydraulic conductivity, intrinsic permeability, and hydraulic diffusivity of the Arbuckle Group. Some of the objectives of this study were to:

- Analyze effects of solid earth tides and atmospheric pressure on water level fluctuations observed in inactive SWD wells.
- Evaluate elastic properties of rocks from horizontal tidal strain and the tidal gravitational potential.
- Compute reservoir parameters from horizontal tidal strain and the tidal gravitational potential.

Chapter 2: Methodology

The motions of the moon and the sun create centrifugal forces or stresses that result in small latitudinal and longitudinal strains in the crust of the Earth (Cutillo and Bredehoeft, 2011). These stresses are known as solid earth tides, which have been long recognized to result in strain in the subsurface and produce corresponding fluctuations in water levels (Cutillo and Bredehoeft, 2011). Using automatic measuring devices, the fluctuations in water levels can be recorded in short-time intervals (Cutillo and Bredehoeft, 2011; Rahi, 2010). Time-series analysis of the fluctuations gives a series of harmonic functions in which tidal components can be identified according to their amplitude (A), frequency (f), and phase relation (Φ) (Cutillo and Bredehoeft, 2011).

The methodology described below was used to evaluate reservoir and rock properties of the Arbuckle Group in northwestern and north-central Oklahoma.

2.1 Pressure Monitoring Instrumentation

Before the deployment of the pressure transducers, baseline monitoring was conducted. Fluid levels and downhole pressure/temperature measurements were taken using a Geotech interface probe and a Calscan Badger+ gauge, respectively. Pressure or fluid level was recorded in 30-second time intervals, since the pressure transducers were deployed. The density of fluid above the pressure transducer was measured during the baseline monitoring using a Calscan Badger+ gauge (Kroll et al., 2017). Pressures can be compensated for atmospheric pressure fluctuations using data from nearby Solinst Barologgers that measure barometric pressure. However, because the Arbuckle is confined by thousands of feet of sedimentary rock in the study area with low

permeability units that form pressure seals, it is a confined reservoir and is not affected by barometric pressure changes.

2.2 Normalization of Data

Inactive Arbuckle SWD wells were instrumented with Solinst Model 3001 LT Levelogger Edge M100:F300 pressure transducers. Using the land surface elevation at the well, well completion measurements, and density of fluid above the pressure transducer, pressure data were normalized to elevation above sea level (m).

2.3 Baseline Trends

An analysis of the uncompensated data was performed to begin the time-series interpretation and analysis. The objective of this step was to identify possible long-term trends that result from regional flow, injection, and seasonal changes. These trends were quantified and corrected for, when necessary, in time-series analyses.

2.4 Tidal Signal

The discrete Fourier transforms technique synthesizes data in sine and cosine functions. For the time series analyses, the software TSoft was used (Van-Camp and Vauterin, 2005). TSoft is an open-source software package for the analysis of time series and Earth tides. The system allows for interactive processing of data with a graphical interface. Each file is stored in a (.txt) text file format and stores information on the location, the instrument used to collect the data, the type of measurement, and the units. The software includes a location database, that allows for the calculation of theoretical tide components for any given latitude, longitude, and ground elevation. The

model for the calculation of the theoretical tide is based on an inelastic non-hydrostatic Earth model. Processing of data, filtering, and evaluation of the spectra using fast Fourier transforms was made with TSoft. With harmonic analysis, the time-series were represented by Fourier series as a regression model. Calculation of Fourier components were plotted against tidal period to produce a periodogram for each well and identify tidal components (Table 1). The frequencies of the tidal components are common to all earth tide data; however, the amplitudes and phase relations for each component are characteristic of each set of tide data (Merritt, 2004). Within this time series analysis, two different harmonic analyses were performed. The first was tidal signal identification, and the second was amplitude and phase angle determination. Both analyses complement each other, and are used to estimate rock and reservoir properties.

Table 1. Five main harmonic components of tides with values compiled from Merritt (2004).

| Symbol | Frequency (cycles per day) | Period (hours) | Explanation |
|----------------|-----------------------------------|-----------------------|------------------------|
| O ₁ | 0.93 | 25.82 | Main lunar diurnal |
| K ₁ | 1.00 | 23.93 | Lunar-solar diurnal |
| M ₂ | 1.93 | 12.42 | Main lunar semidiurnal |
| S ₂ | 2.00 | 12.00 | Main solar semidiurnal |
| N ₂ | 1.90 | 12.66 | Lunar elliptic |

2.5 Computation of properties

Water level fluctuations produced by solid earth tide stresses are a function of some properties of the reservoir, such as specific storage, storage coefficient, transmissivity, porosity, matrix compressibility, and permeability. It is assumed that changes in water level in a well are equal to change in pressure head in the reservoir. The applied stress to the reservoir is absorbed by compression of the pore fluid. Hence, elastic properties and porosity of the reservoir will determine the amplitude of water level response when there is a change in volume.

2.5.1 Specific Storage

The estimation of specific storage (S_s) is achieved from the response of water level fluctuations to earth tides. In Bredehoeft (1967), it was shown that the change in head is produced by the tidal dilatation of the reservoir, which is a function of S_s . Specific storage can be computed if the changes in head can be measured and Poisson's ratio (ν) for the reservoir is known (Bredehoeft, 1967; Cutillo and Bredehoeft, 2011).

The following expression relates S_s (L^{-1}) to tide generating potential (W_2) and changes in head (h):

$$(1) \quad S_s = - \left[\left(\frac{1 - 2\nu}{1 - \nu} \right) \left(\frac{2\bar{h} - 6\bar{l}}{ag} \right) \right] \frac{dW_2}{dh}$$

Where,

ν is the Poisson's ratio for the reservoir material (dimensionless),

\bar{h} and \bar{l} are Love's numbers (constants) used in tidal analysis (dimensionless),

a is the radius of the Earth (L); and

g is acceleration due to gravity (L/T^2).

The negative sign on Eq. 1 indicates that when the tide generating potential (W_2) increases, head in the reservoir decreases (Merritt, 2004). The entire term in brackets in Eq. 1 is a constant.

The tide generating potential (W_2) for Eq. 1 must be predicted from equilibrium tide theory. Using Eq. 2, W_2 can be computed:

$$(2) \quad W_2(\theta, \varphi, t) = gK_m b f(\theta) \cos[\beta(\varphi, t)]$$

Where,

K_m is the general lunar coefficient (L of 53.7 cm), which relates the masses of the earth, the moon, and the earth's radius, and it is obtained from equilibrium tide theory,

b is an amplitude factor that has a distinct value for each tidal component with period (dimensionless). b is obtained from equilibrium tide theory for each harmonic component,

$f(\theta)$ is a latitude function (dimensionless) that will depend on the latitude of each well for each individual harmonic component; and

$\beta(\varphi, t)$ is a phase term (time) that depends on the longitude φ and the Greenwich Mean Time (GMT).

The dimensionless terms b , $f(\theta)$, $\beta(\varphi, t)$ can be obtained for individual harmonic components of the tide, presented on Table 2.

Table 2. Parameters for diurnal and semidiurnal equilibrium tides, from Munk and MacDonald (1960) and Doodson and Warburg (1941)

| Tidal component | b | f(θ) | $\beta(\theta, t)$ |
|------------------------|----------|-------------------------------|---|
| O ₁ | 0.377 | $\sin\theta\cos\theta$ | $qt + \varphi_s(t) - 2\varphi_m(t) - 169.8 \text{ degrees} + \varphi$ |
| K ₁ | 0.531 | $\sin\theta\cos\theta$ | $qt + \varphi_s(t) - 10.2 \text{ degrees} + \varphi$ |
| M ₂ | 0.174 | $0.5\cos^2\theta$ | $2(qt + \varphi_s(t) - \varphi_m(t) - 79.8 \text{ degrees} + \varphi)$ |
| N ₂ | 0.908 | $0.5\cos^2\theta$ | $2(qt + \varphi_s(t) - 1.5\varphi_m(t) + 0.5\varphi_p(t) - 79.8 \text{ degrees} + \varphi)$ |
| S ₂ | 0.423 | $0.5\cos^2\theta$ | $2(qt + \varphi)$ |

Eq. 1 is written as a derivative, but can be approximated by a finite differential of the change in W_2 when head (h) changes by an amount Δh . For the analysis of the tide data set, the ratio of small finite changes (ΔW_2 and Δh) in a small-time period (30 seconds intervals) (Δt) are considered proportional to the ratio of corresponding amplitudes of the theoretical and observed tides. Because some of the components are influenced by both atmospheric and earth tide stresses, using the five main tidal components in Eq. 1 could lead to inaccurate results. For this reason, it is more reliable to use only components O₁ and M₂, which are solely due to solid earth tide stresses with no interaction of atmospheric pressure (Merritt, 2004).

Using the function $A_{2(T, \theta)}$, which is a function of latitude (θ), but not longitude (φ), the amplitude of the harmonic component can be calculated. The amplitude of the harmonic component of W_2 will be defined as $A_{2(T, \theta)}$ and will be replaced in Eq. 1, as follows:

$$(3) \quad S_s = - \left[\left(\frac{1 - 2\nu}{1 - \nu} \right) \left(\frac{2\bar{h} - 6\bar{l}}{ag} \right) \right] \frac{A_2(T, \theta)}{A_h(T)}$$

Where,

T is the period of the harmonic component; and

$A_h(t)$ is the amplitude of a component of the head change of period T

To compute $A_2(T, \theta)$, Eq. 4 will be used.

$$(4) \quad A_2(T, \theta) = gK_m b f(\theta)$$

2.5.2 Storage Coefficient

Storage coefficient is defined as the product of the specific storage and the thickness of the reservoir (Freeze and Cherry, 1979). However, the thickness of the Arbuckle Group at each well is unknown because the top and bottom of the Arbuckle Group have not been well mapped from core or geophysical logs that identify these zones. The thickness of the open interval of each well was used to compute storage coefficient and multiplied by the values of specific storage calculated previously (Eq. 5).

$$(5) \quad S = S_s * b_a$$

Where,

b_a is the thickness of the reservoir (L).

2.5.3 Transmissivity

Oscillations of water levels in a well, as a response of pressure-head disturbance in the reservoir, are a function of periodicity of disturbances, reservoir parameters such as transmissivity and storativity, and inertial and storage effects. The time lag between earth tide dilatation of the reservoir and the water level response in the well was used to estimate aquifer transmissivity. Hsieh et al. (1987) derived an expression to estimate transmissivity of the reservoir. The phase shift (time lag) η will be a function of the transmissivity (T), storage coefficient (S), well radius (r), and periodicity (τ) of the pressure head disturbance (Cutillo and Bredehoeft, 2011).

The dimensionless parameters derived from Hsieh et al. (1987) are:

$$(6) \quad T' = \frac{Tt}{r_c^2}$$

$$(7) \quad S' = \frac{Sr_w^2}{r_c^2}$$

Where,

T' is the redefined transmissivity (dimensionless),

S' is the redefined storage coefficient (dimensionless),

t is the period of the fluctuation of the solid earth tide component ($1/f$),

r_c is the radius of the well casing; and

r_w is the radius of the screened portion of the well.

Using Eq. 6 and Eq. 7, transmissivity can be determined from Figure 4 and Figure 5 and converted into standard units of L^2/T if the phase shift and an order of magnitude of S are known.

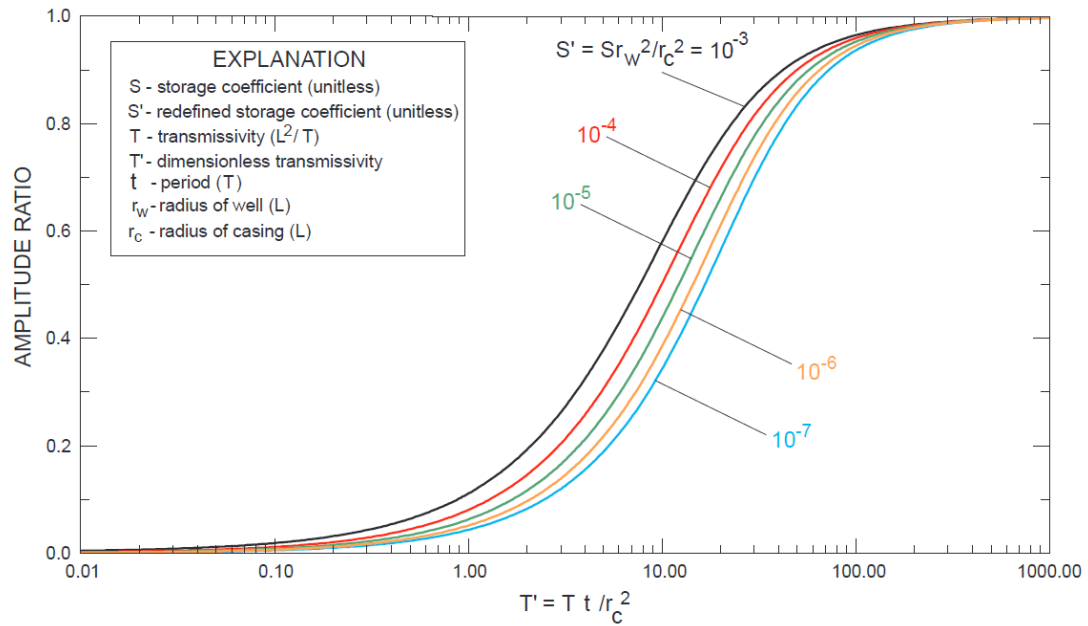


Figure 4. Ratio of amplitudes of the well water level and reservoir pressure head oscillations as a function of dimensionless transmissivity, from Merritt (2004).

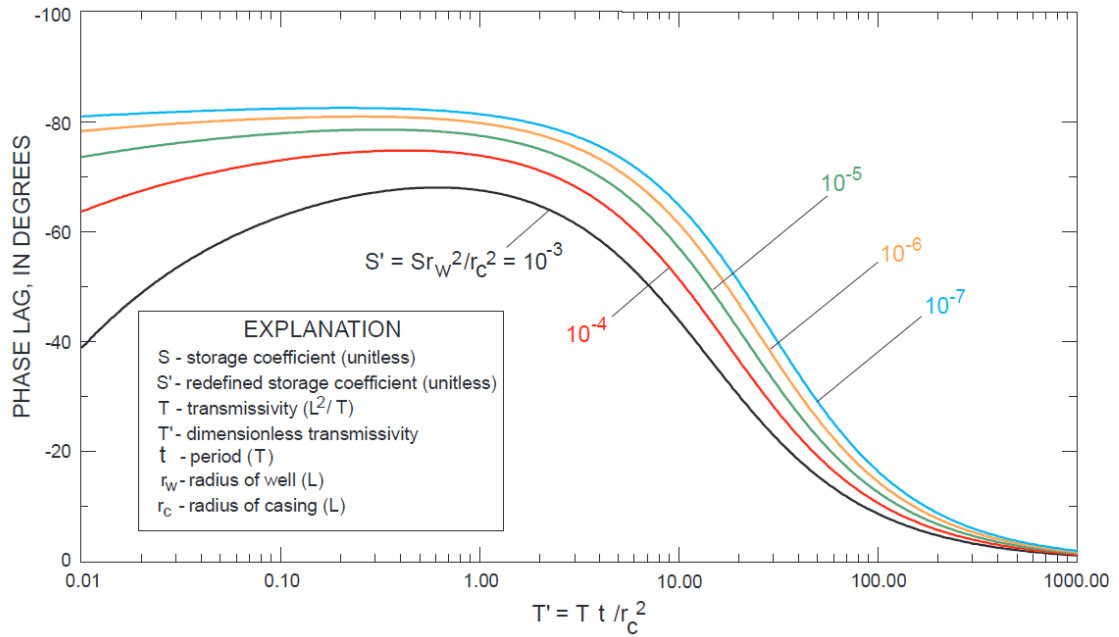


Figure 5. Phase lag between the well water-level and reservoir pressure head oscillations as a function of dimensionless transmissivity, from Merritt (2004).

2.5.4 Matrix Compressibility

Acworth et al. (2015) showed that if we assume undrained conditions for the reservoir apply for the frequencies involved, we can define barometric efficiency (BE) as:

$$(8) \quad BE = 1 - \gamma$$

Where,

γ is the loading efficiency.

We can express the loading efficiency of the reservoir as a relationship between fluids compressibility, porosity calculated from BE, and compressibility of the material (β) (Eq. 9).

$$(9) \quad \gamma = \frac{\alpha}{\phi\beta_w + \alpha}$$

Where,

α is the matrix compressibility,

β_w is the fluid compressibility,

and ϕ is porosity.

Rearranging Eq. 9, we can obtain values of matrix compressibility for the reservoir, having already calculated barometric efficiency and porosity (Acworth et al., 2015).

2.5.5 Hydraulic Conductivity

Hydraulic conductivity (K) is a function of the porous medium and the fluid (Freeze and Cherry, 1979). Being a function of both properties, the hydraulic conductivity refers to the rate at which water will move through a porous medium. A relatively higher viscosity water (e.g., brine) will be transmitted through a porous medium at a slower rate than a relatively lower viscosity water (e.g., freshwater). Hydraulic conductivity was computed from the transmissivity (L^2/T) divided by the aquifer thickness to obtain a value in terms of L/T .

2.5.6 Intrinsic Permeability

Intrinsic permeability (k_i) is a function of the porous medium alone and it refers to the material to transmit fluid (Fetter, 2013). Intrinsic permeability was computed from the values obtained of hydraulic conductivity using Eq. (10).

$$(10) \quad k_i = \frac{K\mu}{\rho_w g}$$

Where,

μ is the dynamic viscosity of brine,

ρ_w is the density of brine, and

g is acceleration due to gravity.

2.5.7 Hydraulic Diffusivity

Hydraulic diffusivity is a measure of the rate at which fluid can spread through a material, and is represented as the ratio of transmissivity to storage coefficient (Freeze and Cherry, 1979), so was computed from the properties obtained in previous steps. Higher permeability allows for higher fluid velocities and, therefore, faster spreading or migration of fluid pressure. Higher storage coefficient allows more fluid to be stored in the porous medium per unit change in head; therefore, higher storage coefficients result in slower spreading or migration of fluid pressure (Keranen et al., 2014).

2.6 Barometric Efficiency

The Leveloggers are not vented, hence barometric efficiency was calculated to determine if uncompensated or compensated data should be used for time-series

analysis. The objective of this calculation was to evaluate whether the data needs to be compensated in a 30 second time interval or if the data needs to be changed to terms of absolute pressure from gauge pressure using the average of the barometric pressure.

Barometric efficiency (BE) is a useful tool to compute porosity of a confined aquifer after having calculated specific storage from tidal strain. It is defined as the ratio of the aquifer pressure head change to the atmospheric pressure change (Rahi, 2010). Barometric efficiency was computed from the approach found in Acworth et al. (2015) and computes BE from theoretical tide strain and the tide components in the continuous data.

Using the amplitude of the components O_1 , M_2 , and S_2 of the earth tide strain in the water level record and the theoretical tide, a first estimate of barometric efficiency was computed. It was demonstrated that barometric efficiency of an aquifer can be calculated from the ratio of the aquifer response to the atmospheric pressure change that drives the corresponding response. The S_2 component of solid earth tides has part of the solid earth tide and atmospheric pressure. Therefore, the hydraulic head response to S_2 component has two parts (Eq. 11).

$$(11) \quad S_{2h} = S_{2h-a} + S_{2h-earth}$$

Where,

S_{2h-a} is the input from the atmospheric tide and,

$S_{2h-earth}$ is the input from the solid earth tide.

The barometric efficiency is computed from the ratio of S_{2h-a} to S_{2h} . The value for S_{2h} was obtained by first finding the value of $S_{2h-earth}$ using amplitudes of the

components S_2 and M_2 in the theoretical tide strain calculated in TSoft (Figure 6) (Van-Camp and Vauterin, 2005). Then, multiplying the ratio of S_2 to M_2 by the amplitude of the M_2 component in the water level record we can obtain a value for $S_{2h-earth}$ (Eq. 11 and Eq. 12).

$$(12) \quad S_{2h-earth} = \frac{S_2}{M_2} M_{2h}$$

Where,

S_2 and M_2 are the amplitudes of the tidal components in the theoretical tidal strain and,

M_{2h} is the amplitude of component M_2 in the water level record.

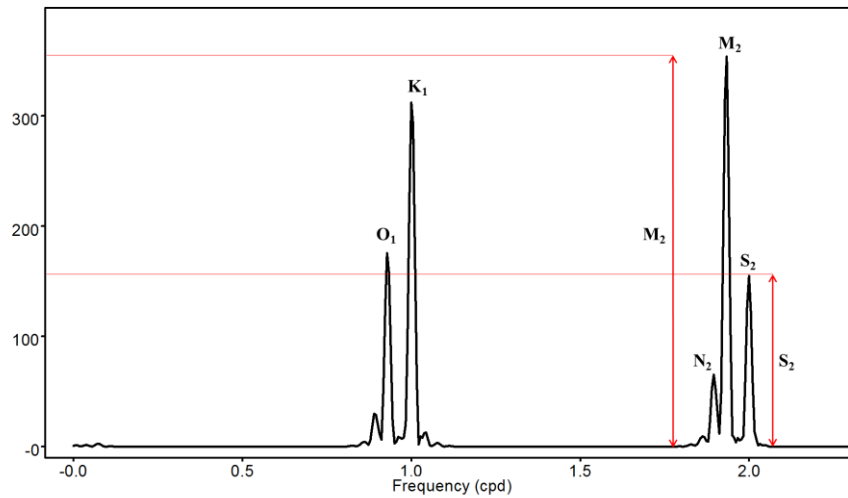


Figure 6. Amplitudes of M_2 and S_2 components in the theoretical tidal strain for well Alfalfa 03 to calculate $S_2:M_2$ ratio.

Having $S_{2h-earth}$ and the amplitude of S_{2h} from the water level record, S_{2h-a} was computed from Eq. 11. With Eq. 13, the barometric efficiency was calculated.

$$(13) \quad BE = \frac{S_{2h-a}}{S_{2h}}$$

2.7 Reservoir Porosity

The porosity can be computed using the barometric efficiency estimated from the methods explained above. Eq. 14 relates porosity and specific storage as follows:

$$(14) \quad \eta = \frac{B_e S_s}{\beta_w g \rho_w}$$

Where,

η is porosity (dimensionless),

B_e is barometric efficiency (dimensionless)

S_s is specific storage (m^{-1})

β_w is compressibility of water (ms^2/kg); and

ρ_w is density of water (kg/m^3)

g is acceleration due to gravity (m/s^2)

The compressibility of water and weight density of water were obtained for values of brine with approximately 150,000 ppm, which is a value typical for saltwater (Murray and Holland, 2014).

Chapter 3: Present Study

3.1 Introduction

Solid earth tides stress inland confined aquifers causing water level fluctuations. Since the mid-20th century, hydrologists have been refining techniques to obtain aquifer and rock properties from water level fluctuations as a response to earth tides (Bredehoeft, 1967; Cutillo and Bredehoeft, 2011; Hsieh et al., 1987). Evaluation of the water level fluctuations due to solid earth tides as time series is used to estimate aquifer properties such as specific storage, storage coefficient, transmissivity, porosity, matrix compressibility, and permeability (Bernard and Delay, 2008; Bredehoeft, 1967; Cutillo and Bredehoeft, 2011; Mehnert et al., 1999). Water level fluctuations as a response to solid earth tides constitute a very useful tool to obtain aquifer properties in aquifers where it is not practical to do an aquifer or slug test (Cutillo and Bredehoeft, 2011).

The Arbuckle Group is an important geologic unit of Cambrian to Early Ordovician age composed mainly of carbonates (Johnson, 1991; Ragland and Donovan, 1991). The Arbuckle Group has been used as a saltwater disposal (SWD) zone by the oil and gas industry in Oklahoma. In 2014, the Arbuckle Group received about 68% of the total volumes of saltwater disposed in the state of Oklahoma (Murray, 2015). In the last years, induced seismicity has brought attention to the Arbuckle Group, since some studies suggest that increases in saltwater injection into the Arbuckle Group is linked to increase in the number and magnitude of earthquakes occurring in Oklahoma (Keranen et al., 2013; Keranen et al., 2014; Weingarten, 2015; Weingarten et al., 2015; Witze, 2015). Despite the importance of the Arbuckle Group as a SWD zone and induced seismicity, the hydraulic parameters of the Arbuckle Group have not been widely

studied or were studied in association with the Simpson Group, since both units comprise the Arbuckle-Simpson Aquifer in south-central Oklahoma (Christenson et al., 2009; Christenson et al., 2011).

In this study, water level and barometric pressure records have been measured at six deep, inactive, Arbuckle SWD wells located in the Anadarko Shelf and Cherokee Platform in Alfalfa, Grant, Lincoln, Logan, and Pawnee Counties in Oklahoma. Downhole pressure was monitored in the wells beginning in August 2016. The open intervals of the wells are in the Arbuckle Group and, in most cases, have no observed effects or stresses from production or injection; therefore, water level fluctuations are largely due to earth tides.

3.2 Objectives

Analysis of water level fluctuations as a result of tidal strain was used to estimate reservoir properties for the Arbuckle Group in northwestern and north-central Oklahoma. The main purpose of this study was to calculate specific storage, storage coefficient, transmissivity, porosity, matrix compressibility, and permeability of the Arbuckle Group using spectral analysis of time series and application of fast Fourier transforms. The objective was achieved by analyzing effects of solid earth tides and atmospheric pressure on water level fluctuations in inactive SWD wells; evaluating elastic properties and reservoir properties from horizontal tidal strain and tidal gravitational potential.

3.3 Materials and Methods

Continuous measurements, with pressure transducers, of water levels was necessary to observe short time-frequency fluctuations and then compute the reservoir and rock properties of the Arbuckle Group. Prior to the deployment of the pressure transducers, baseline monitoring of fluid levels, downhole pressure, and temperature were measured using a Geotech interface probe and a Calscan Badger+ gauge. After deployment, pressure or fluid level was recorded in 30-second time intervals using Solinst Model 3001 LT Levelogger Edge M100:F300 pressure transducers. Data from the pressure transducers was normalized to meters above sea level using land surface elevation at the well, well completion measurements, and density of fluid above the pressure transducer. Atmospheric pressure was observed on 30-second time intervals with Solinst Barologgers so that it could later be used for calculating barometric efficiency.

With the measurement, computations of properties were achieved using time series analysis and fast Fourier transforms. Data for fluid elevation in meters above sea level (msl) was filtered using a FFT bandpass filter with cutoff frequency of 1.5 cycles per day (cpd) and a band width of 1 cpd to contain the signals of the tidal components at 1 and 2 cpd (Table 1). The filter eliminated possible baseline trends and retrieved the water level fluctuation measurements as a series of signals with the form of the expected signal for solid earth tides (Figure 7). The fluid elevation, filtered data, and theoretical tidal strain for each well is presented in Appendix A.

After applying a bandpass FFT filter in the fluid elevation data, an evaluation of the spectrum was performed to obtain the amplitudes of each tidal component in the

water level measurement (Figure 8). Amplitudes for O_1 tidal component were obtained using a bandpass FFT filter with the frequency of the component as the cut-off frequency and a band width of 0.01 cpd to avoid computing the signal from component K_1 and possible biased results. The frequency spectrum for the observed and theoretical solid earth tide of each well is presented in Appendix B.

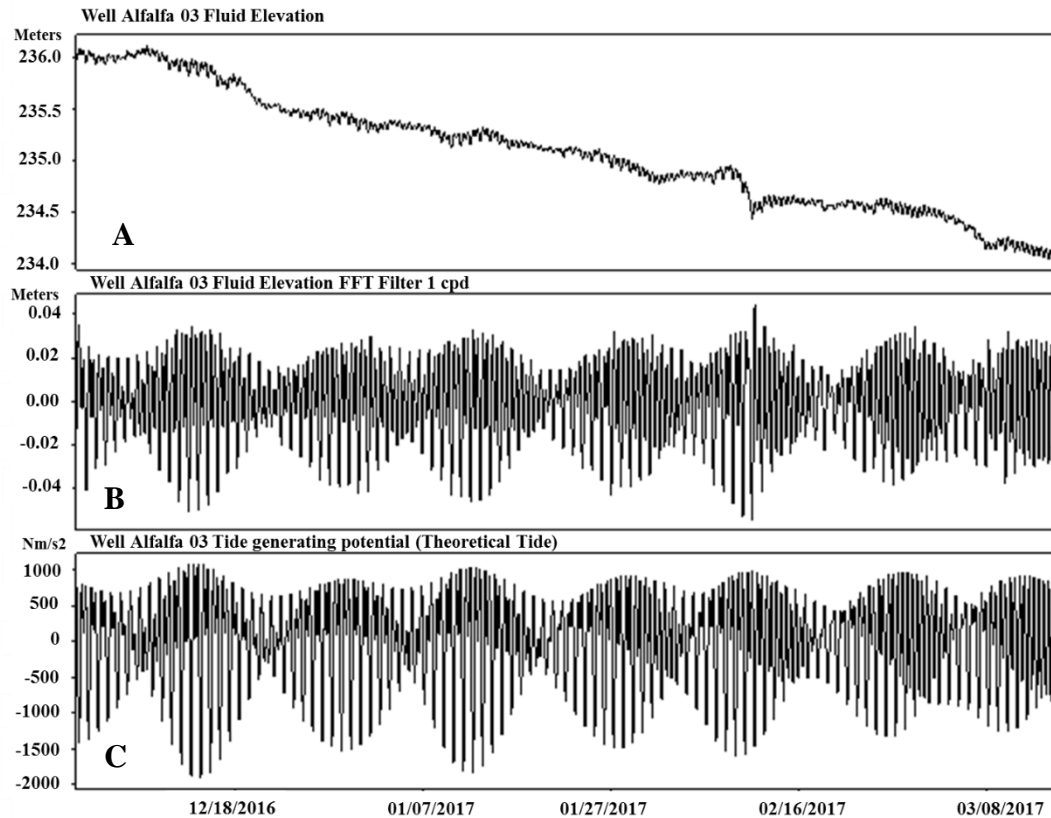


Figure 7. Time series for the well Alfalfa 03. Fig 7a. shows the water level fluctuations measurement. Fig 7b. shows the filtered data (FFT band pass filter cutoff frequency 1.5 cpd and band width 1 cpd). Fig 7c. shows the theoretical tide generating potential.

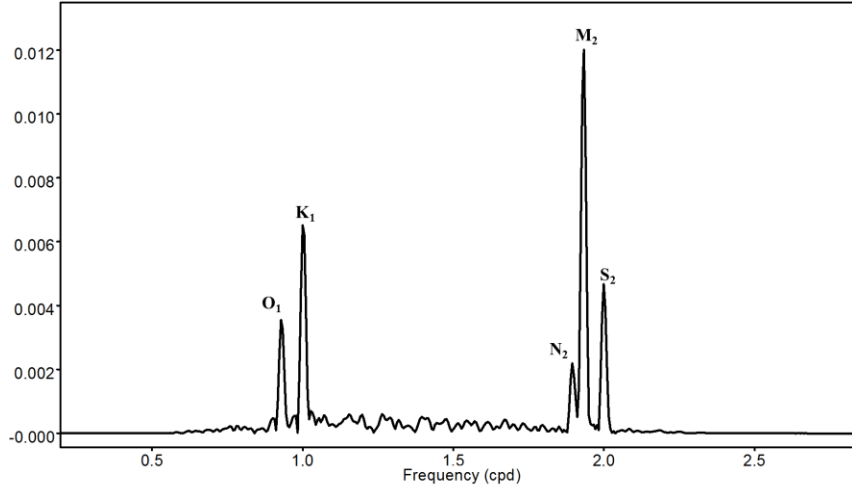


Figure 8. Spectrum of tidal components in filtered data from well Alfalfa 03. Each tidal component is identified.

3.3.1 Estimation of Specific Storage

Bredehoeft (1967) showed that the change of head is a response of the dilatation of the reservoir product of tidal strain, and that change of head is a function of specific storage (S_s). Using the changes in head in the well and knowing Poisson's ratio (ν), S_s was computed (Bredehoeft, 1967; Cutillo and Bredehoeft, 2011; Merritt, 2004).

Eq. 15 relates S_s to tide generating potential (W_2) and changes in head (h):

$$(15) \quad S_s = - \left[\left(\frac{1-2\nu}{1-\nu} \right) \left(\frac{2\bar{h} - 6\bar{l}}{ag} \right) \right] \frac{dW_2}{dh}$$

Typical values used for Poisson's ratio (ν) for confined aquifers is 0.25 and Love's numbers (\bar{h}) and (\bar{l}) are 0.6 and 0.07, respectively. The term a is the radius of the earth (6.371 E08 cm) and g is the acceleration due to gravity (979 cm/s²). Therefore, the term in the brackets in Eq. 15 is a constant. The tide generating potential was predicted with equilibrium tide theory using Eq. 16.

$$(16) \quad W_2(\theta, \varphi, t) = gK_m b f(\theta) \cos[\beta(\varphi, t)]$$

Eq. 16 is a constant where g is acceleration due to gravity (979 cm/s^2), K_m is the general lunar coefficient (53.7 cm), b is a constant value defined for each component, $f(\theta)$ is a function of the latitude of each well, and $\cos[\beta(\phi,t)]$ is a function of latitude, longitude, and time (Table 2). Eq. 15 is written as a derivative; however, it can be approximated by a finite differential. For the analysis of the data sets, the ratio of small infinite changes in tide generating potential (ΔW_2) and head (Δh) are proportional to the ratio of corresponding amplitudes of the theoretical and observed tides. In groundwater studies, it is most common to use the tidal components O_1 and M_2 , since they do not have interactions with atmospheric pressure and are completely caused by solid earth tides stresses (Cuttillo and Bredehoeft, 2011; Merritt, 2004). Therefore Eq. 14 becomes Eq. 17.

$$(17) \quad S_s = - \left[\left(\frac{1-2\nu}{1-\nu} \right) \left(\frac{2\bar{h} - 6\bar{l}}{ag} \right) \right] \frac{A_2(T, \theta)}{A_h(T)}$$

To calculate the amplitude of the theoretical tide components, Eq. 18 was used.

$$(18) \quad A_2(T, \theta) = gK_m b f(\theta)$$

The amplitude of each tidal component was computed from Eq. 18, which is an equation dependent on the latitude of the well. Amplitude of each tidal component in the observed tide was estimated using TSoft (Van-Camp and Vauterin, 2005) and fitting a tidal model to the water level fluctuations observed.

3.3.2 Estimation of Storage Coefficient

With specific storage determined from the amplitudes of theoretical and observed tides, the storage coefficient (S) was computed by multiplying the thickness of the open interval portion of each well (b_a) by S_S (Eq. 19). Since the top and bottom of the Arbuckle Group are not well mapped in Oklahoma, the open interval of each well gave an estimate of the thickness of the reservoir.

$$(19) \quad S = S_S * b_a$$

3.3.3 Estimation of Transmissivity

The time lag between earth tide dilatation of the reservoir and the water level response in the well was used to estimate transmissivity (T). Hsieh et al. (1987) derived an expression to estimate transmissivity of a reservoir. Using the storage coefficient (S), the radius of the well r_w , and the radius of the casing r_c , a value of redefined storage coefficient (S') was computed (Eq. 20).

$$(20) \quad S' = \frac{S r_w^2}{r_c^2}$$

Where,

S' is redefined storage coefficient (dimensionless),

r_w^2 is radius of the well (L^2),

r_c^2 is radius of the casing (L^2)

The redefined storage coefficient (S') was plotted in a series of graphs using the amplitude ratio or the phase lag between the water level and reservoir pressure head oscillations (Figure 4 and Figure 5). The value obtained had units of dimensionless

transmissivity (T'). Using Eq. 21, a value for transmissivity (L^2/T) was calculated for the reservoir.

$$(21) \quad T' = \frac{Tt}{r_c^2}$$

Where,

T' is dimensionless transmissivity,

T is transmissivity (L^2/T), and

t is period of the tidal component (T)

3.3.4 Estimation of Matrix Compressibility

Matrix compressibility (β) was computed assuming undrained conditions for the reservoir that apply the frequencies involved in the observed solid earth tides.

Barometric efficiency (BE) can also be expressed $BE=1-\gamma$, where γ is the loading efficiency. Eq. 22 relates the loading efficiency with fluids compressibility, porosity, and matrix compressibility.

$$(22) \quad \gamma = \frac{\alpha}{\phi\beta_w + \alpha}$$

Rearranging the terms in Eq. 22, matrix compressibility was computed for the Arbuckle Group.

3.3.5 Estimation of Barometric Efficiency

Barometric efficiency (BE) is a useful tool to compute porosity of a confined aquifer after having calculated specific storage from tidal strain. It is defined as the ratio

of the aquifer pressure head change to the atmospheric pressure change (Rahi, 2010). Two different methods were used to compute barometric efficiency from the barometric pressure and the water level measurements.

Using the amplitude of the components O_1 , M_2 , and S_2 of the earth tide strain in the water level record and the theoretical tide, a first estimate of barometric efficiency was computed. The S_2 component of solid earth tides has part of the solid earth tide ($S_{2h-earth}$) and atmospheric pressure (S_{2h-a}). Therefore, the hydraulic head response to S_2 component has two parts (Eq. 23).

$$(23) \quad S_{2h} = S_{2h-a} + S_{2h-earth}$$

The barometric efficiency is computed from the ratio of S_{2h-a} to S_{2h} . To obtain the value for S_{2h} , the value of $S_{2h-earth}$ must be found first. This value can be obtained from the amplitudes of the components S_2 and M_2 in the theoretical tide strain. Then, multiplying the ratio of S_2 to M_2 by the amplitude of the M_2 component in the water level record we can obtain a value for $S_{2h-earth}$. Having $S_{2h-earth}$ and the amplitude of S_{2h} from the water level record, S_{2h-a} was computed from Eq. 22. With Eq. 24, the barometric efficiency was calculated.

$$(24) \quad BE = \frac{S_{2h-a}}{S_{2h}}$$

3.3.6 Estimation of Porosity

With barometric efficiency estimated, the porosity can be computed. Eq. 25 relates porosity (η), specific storage (S_s), compressibility of water (β_w), and density of water (ρ_w). Values for β_w and ρ_w were obtained for brine with TDS of approximately

150,000 ppm, which is a value typical for brine in Oklahoma reservoirs (Murray and Holland, 2014).

$$(25) \quad \eta = \frac{B_e S_S}{\beta_w \rho_w}$$

3.3.7 Hydraulic Conductivity

Hydraulic conductivity (K) is a function of the porous medium and the fluid (Freeze and Cherry, 1979). Hydraulic conductivity was computed from the transmissivity (L^2/T) divided by the aquifer thickness (L) to obtain a value in terms of L/T .

3.3.8 Intrinsic Permeability

Intrinsic permeability (k_i) is a function of the porous medium alone (Fetter, 2013). Intrinsic permeability was computed from the values obtained for hydraulic conductivity using Eq. (26).

$$(26) \quad k_i = \frac{K\mu}{\rho_w g}$$

Where,

μ is the dynamic viscosity of brine,

ρ_w is the density of brine, and

g is acceleration due to gravity.

3.3.9 Hydraulic Diffusivity

Hydraulic diffusivity is a measure of the rate at which fluid can spread through a material, and is represented as the ratio of transmissivity to storage coefficient (Freeze

and Cherry, 1979), so was computed from the properties obtained in previous steps. Higher permeability allows for higher fluid velocities and, therefore, faster spreading or migration of fluid pressure. Higher storage coefficient allows more fluid to be stored in the porous medium per unit change in head; therefore, higher storage coefficients result in slower spreading or migration of fluid pressure (Keranen et al., 2014).

3.4 Results and Discussion

Time series analyses of the water level fluctuations showed that all the studied wells respond to solid earth tide stresses. Therefore, it was possible to estimate rock properties for the Arbuckle Group from the fluid level response. The amplitudes of the fluctuations obtained for O_1 and M_2 components and the lag in time (phase shift) are a function of the reservoir material and hydrologic properties of Arbuckle Group. Table 3 presents the measured amplitudes and phase shifts for O_1 and M_2 tidal components in the observed solid earth tides for the wells.

Wells Alfalfa 04 and Grant 06 present noise in the data, which can be a product of other processes interfering with the water level fluctuations. The interference can be observed in the anomalous phase shifts obtained for the tidal components. To avoid said interferences that bias the data, a bandpass FFT filter with a band width of 0.01 cpd was applied to the specific frequencies of O_1 and K_1 components to retrieve the amplitude for O_1 without interference from K_1 .

Table 3. Amplitudes and lags in time for the tidal components O₁ and M₂ in the water level record for the studied wells.

| Well ID | Tidal component | Amplitude (m) | Phase shift (degrees) |
|------------|-----------------|---------------|-----------------------|
| Alfalfa 03 | O ₁ | 0.0054 | 91.42 |
| | M ₂ | 0.0130 | 169.95 |
| Alfalfa 04 | O ₁ | 0.0030 | 75.50 |
| | M ₂ | 0.0037 | 156.73 |
| Grant 06 | O ₁ | 0.0030 | 46.38 |
| | M ₂ | 0.0037 | 135.66 |
| Lincoln 10 | O ₁ | 0.0032 | 88.75 |
| | M ₂ | 0.0053 | 160.08 |
| Pawnee 11 | O ₁ | 0.0055 | 85.08 |
| | M ₂ | 0.0140 | 178.92 |
| Logan 12 | O ₁ | 0.0039 | 88.46 |
| | M ₂ | 0.0110 | -179.71 |

3.4.1 Specific Storage

Specific storage (S_s) is defined as the volume of water that an aquifer expels or absorbs when the pressure head decreases or increases by a unit amount from a unit volume (Fetter, 2013). Computed specific storage values ranged from $3.38 \text{ E-}07 \text{ m}^{-1}$ to $2.66 \text{ E-}06 \text{ m}^{-1}$ with a median of $1.39 \text{ E-}06 \text{ m}^{-1}$. These values are one order of magnitude lower than previous values reported in studies of the Arbuckle-Simpson Aquifer. However, the portion of the Arbuckle Group in the study area is confined and only evaluates the Arbuckle Group, and not the mixed zone of the Arbuckle Simpson Aquifer. The estimates based on the O₁ and M₂ tidal components appear to be consistent in each monitoring zone for the Arbuckle Group. As well, textbook values for confined aquifers are consistent with specific storage values obtained for the Arbuckle Group in the study area. Figure 9 presents the range of values for S_s including a comparison to

previous values estimated for the Arbuckle-Simpson Aquifer and textbook values for confined calcareous aquifers.

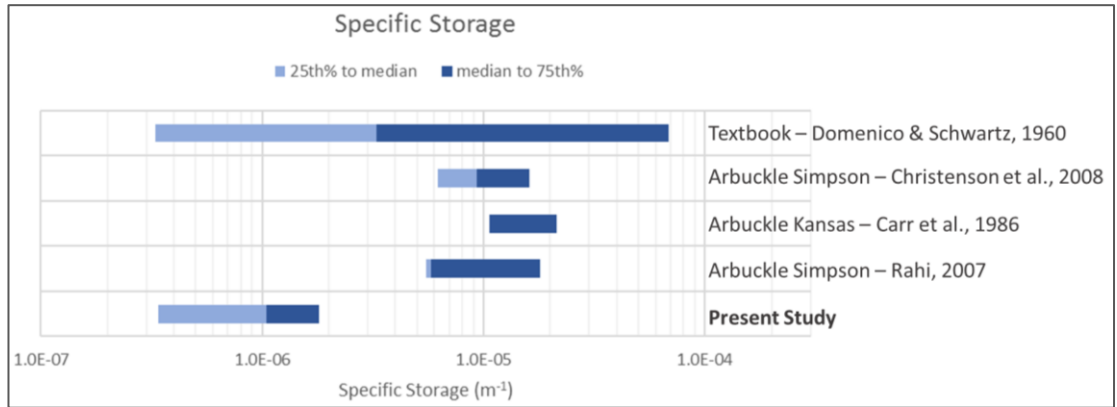


Figure 9. Range of S_s computed values from solid earth tide analyses (present study) and comparison from previous studies.

3.4.2 Storage Coefficient

The storage coefficient (S), also known as storativity, refers to the volume of water an aquifer releases from or takes into storage from a decrease or increase of one unit in head from a unit surface area (Fetter, 2013). Storage coefficient values computed from the estimates of S_S ranged from 5.67 E-05 to 2.57 E-03, with a median of 3.69 E-04 (dimensionless parameter). Typical values for a confined reservoir range from E-03 to E-05 (Todd, 1980). The values of storage coefficient are one to two orders of magnitude lower than previously reported values for the Arbuckle Group or the Arbuckle-Simpson Aquifer (Figure 10). The difference in the values are a function of the thickness of the unit for the computation of the property and the unconfined, semi-confined, or confined nature of the unit in the study area. Previous studies for the Arbuckle-Simpson Aquifer were conducted in semi-confined portions of the aquifer

where the Arbuckle Group has a larger thickness and the thickness of the Simpson Group was considered as well.

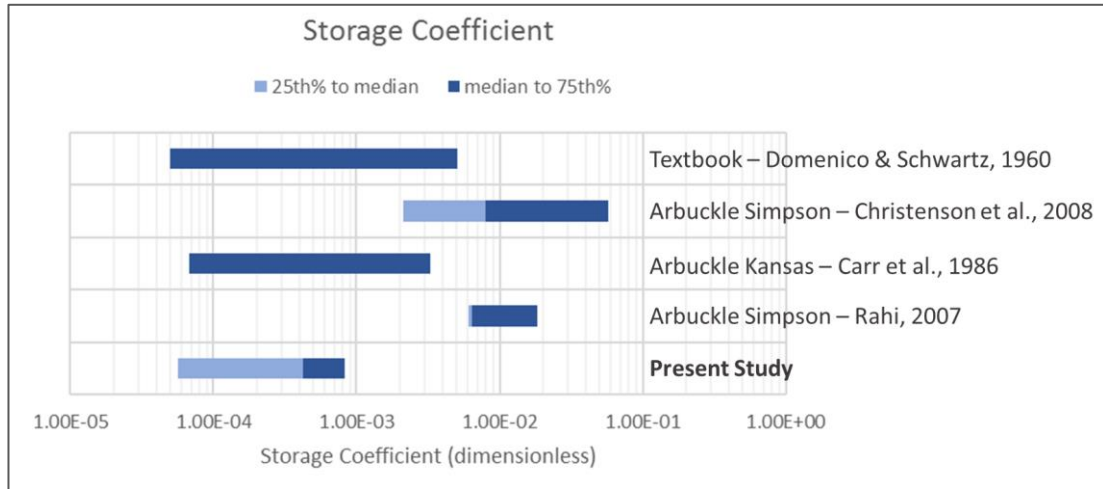


Figure 10. Range of S computed values from solid earth tide analyses (present study) and comparison from previous studies.

3.4.3 Transmissivity

The transmissivity (T) is defined as the rate at which water is transmitted through a unit width of porous medium under a unit hydraulic gradient. It is a function of the liquid (viscosity and density), the porous media, and the thickness of the porous media (Fetter, 2013). From the method developed by Hsieh et al. (1987), the redefined storage coefficient (S') was computed using the radius of production and radius of the wells. Redefined storage coefficient ranged from 4.12 E-05 to 1.85 E-03 with a median value of 4.68 E-04. Using the graphs from the approach made by Hsieh et al. (1987) and the amplitude ratios of the components O₁ and M₂ in the water level records it was possible to calculate dimensionless transmissivity and then convert it to transmissivity in units of L²/T. The values of transmissivity range from 2.09 m²/d to 375.48 m²/d.

Figure 12 presents the range of computed transmissivity and comparison to previous values reported for the Arbuckle Simpson Aquifer. Values of transmissivity were computed from the storage coefficient using the redefined storage coefficient, therefore they are a function of the thickness of the reservoir. Thickness of the Arbuckle Simpson Aquifer is greater than the thickness of the Arbuckle Group in the study area.

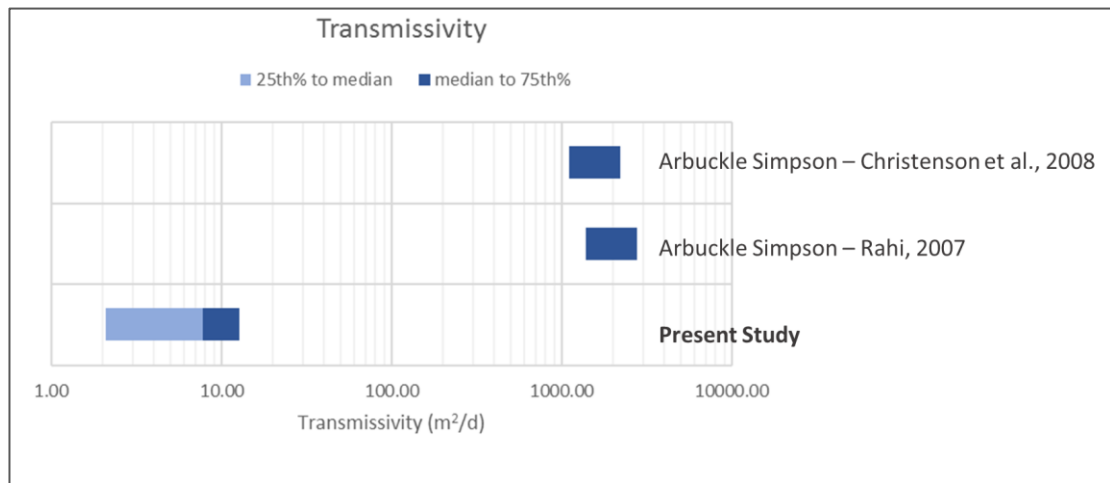


Figure 11. Range of T computed values from solid earth tide analyses (present study) and comparison to previous studies.

3.4.4 Matrix Compressibility

Values of matrix compressibility were computed using the values of barometric efficiency and porosity. The values of matrix compressibility range from $9.26 \text{ E-}08 \text{ psi}^{-1}$ to $6.18 \text{ E-}07 \text{ psi}^{-1}$, with a median value of $3.02 \text{ E-}07 \text{ psi}^{-1}$. Figure 12 presents the range of values for matrix compressibility computed for this study and compares them to reservoir engineering textbook compressibility ranges. The value used for fluid compressibility was calculated for brine with approximately 150,000 ppm of TDS, a typical value for saltwater of the Arbuckle Group ($2.67 \text{ E-}07 \text{ psi}^{-1}$). There were not

estimates of matrix compressibility for the Arbuckle Group in previous studies. However, the values obtained in this study are consistent with values of matrix compressibility for confined calcareous reservoirs like the Arbuckle Group.

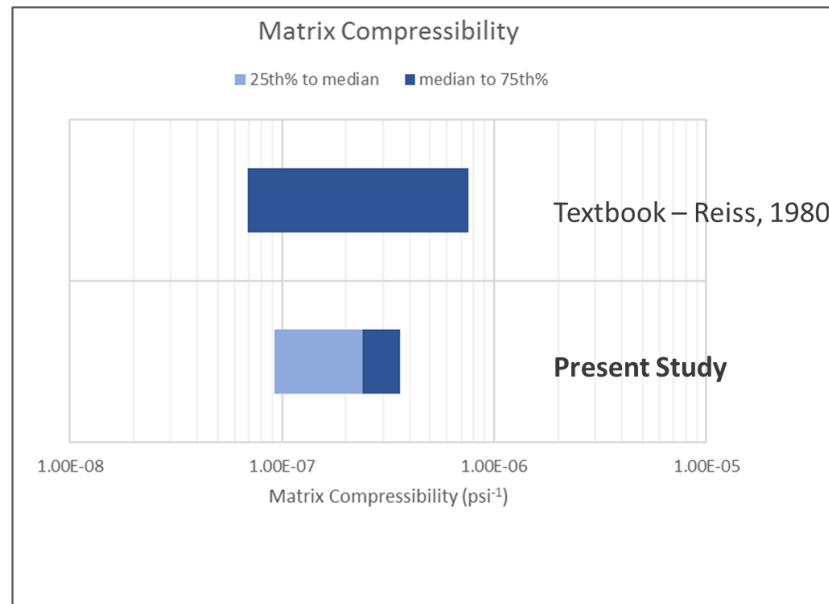


Figure 12. Range of α computed values from solid earth tide analyses (present study) and comparison to textbook value.

3.4.5 Barometric Efficiency

Barometric efficiency for the wells was computed by the methods described in Acworth et al. (2015) (Section 3.3.5). Calculated barometric efficiency ranges from 0.42 to 0.87. For confined aquifers, the values of barometric efficiency must be close to 1 or 1 (Acworth et al., 2015; Rahi, 2010). The values of barometric efficiency computed are consistent with expected values for a confined aquifer, as they are close to 1. Figure 13 presents the range of values for barometric efficiency for this study. Only one other previous study for the Arbuckle Simpson Aquifer in south-central Oklahoma computed

values of barometric efficiency. The median of the values reported for Rahi (2010) is lower than the present study. In Rahi (2010), portions of the Arbuckle Simpson Aquifer studied were semi-confined to confined. Lower values of barometric efficiency correspond to semi-confined portions of the aquifer.

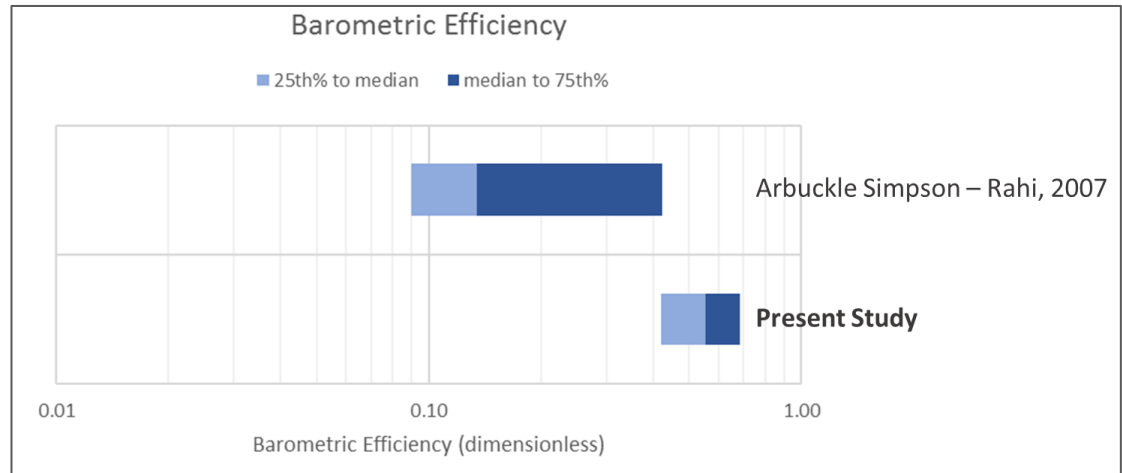


Figure 13. Range of BE computed values from solid earth tide analyses (present study) and comparison from previous studies.

3.4.6 Reservoir Porosity

The porosity values computed for the Arbuckle Group in the monitoring wells ranged from 5% to 54%, with an median value of 24%. Freeze and Cherry (1979) estimate values of porosity ranging from 2% to 50% for karst and cavernous limestone. Previous diagenetic studies of the Arbuckle Group have shown that there is karstification and vuggy porosity in the dolomites of the unit, which can account for the values of porosity of 54% computed in the present study. Figure 14 presents the porosity values computed for the studied wells and comparison to textbook values and textbook values.

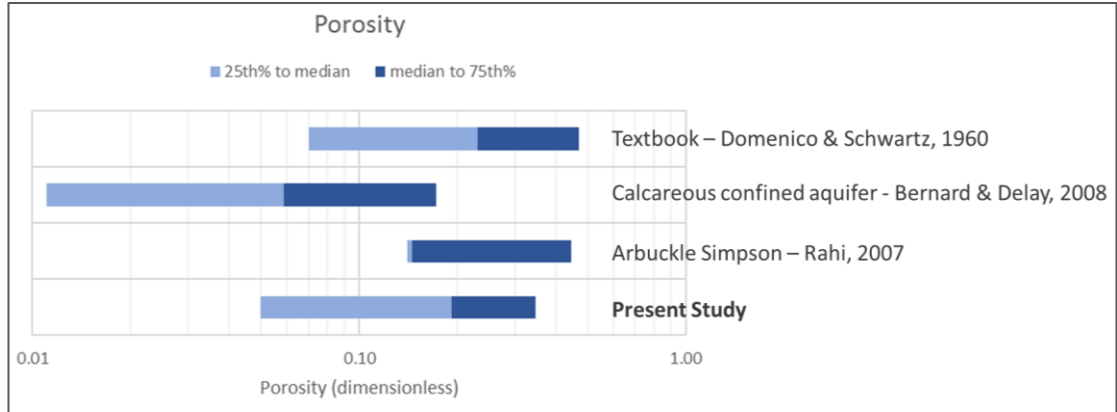


Figure 14. Range of η computed values from solid earth tide analyses (present study) and comparison from previous studies.

3.4.7 Hydraulic Conductivity

Hydraulic conductivity was computed from the transmissivity divided by the thickness of the open interval of the wells. Hydraulic conductivity refers to rate at which water will move through a porous medium. For confined reservoirs made of dolomite and limestone, hydraulic conductivity can range from E-05 to E-08 m/s (Freeze and Cherry, 1979). Values of hydraulic conductivity computed for the wells ranged from 7.90 E-08 m/s to 9.78 E-06 m/s, with a median value of 2.21 E-07 m/s. Figure 15 presents the ranges of hydraulic conductivity values for the present study and comparison to textbook values and previous Arbuckle Simpson Aquifer studies. The values from Christenson et al. (2011) from south-central Oklahoma are widely used in hydrogeological models for saltwater injection and induced seismicity in north-central Oklahoma, for example, a study by Keranen et al. (2014).

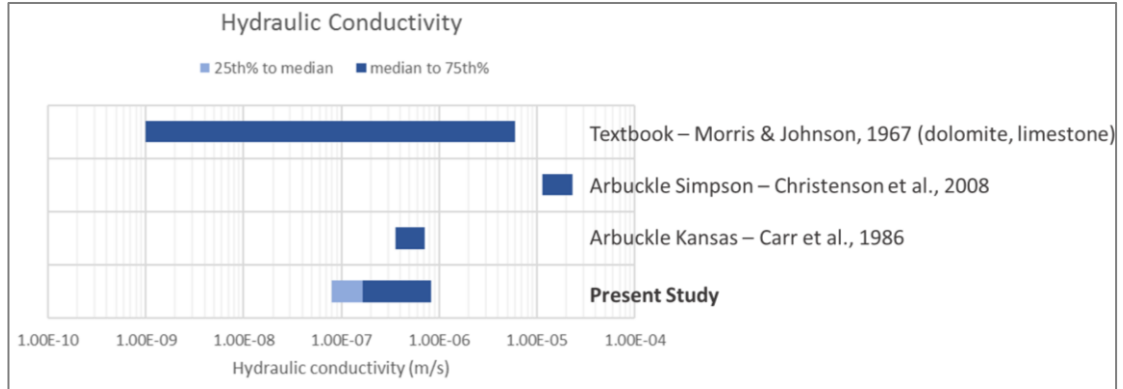


Figure 15. Range of K computed values from solid earth tide analyses (present study) and comparison to previous studies.

3.4.8 Intrinsic Permeability

Intrinsic permeability was computed from the hydraulic conductivity and dynamic viscosity and density of brine with total dissolved solids of 150,000 ppm, common value for brines. Values of intrinsic permeability ranged from 12.29 mD (millidarcy) to 1.5 D (Darcy). According to Freeze and Cherry (1979), values for intrinsic permeability for limestones and dolomites range from 0.001 to 1 D. Figure 16 presents ranges for intrinsic permeability for this study and a comparison to values of intrinsic permeability from previous studies.

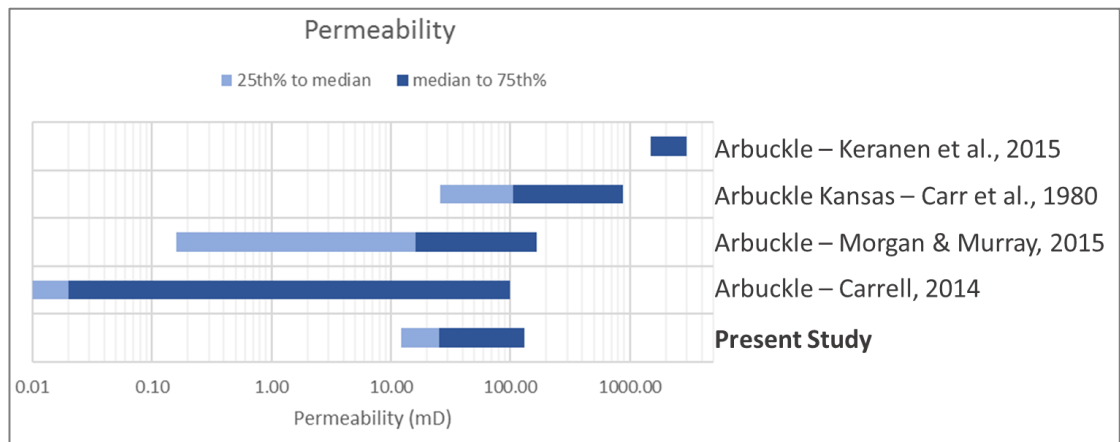


Figure 16. Range of k_i computed values from solid earth tide analyses (present study) and comparison from previous studies.

3.4.9 Hydraulic Diffusivity

Hydraulic diffusivity is represented as the ratio of transmissivity to storage coefficient. It is a measure of the rate at which fluid can spread through a material and is represented as the ratio of transmissivity to storage coefficient. Values of hydraulic diffusivity computed from the solid earth tide time series analyses ranged from 0.04 m²/s to 4.91 m²/s, with a median value of 0.69 m²/s. Figure 17 presents values of hydraulic diffusivity from the present study and comparison to two other studies on the Arbuckle Group. In the Keranen et al. (2014) hydrogeologic model, they use a hydraulic diffusivity of 2 m²/s and test different hydraulic diffusivities for the injection scenarios. Their median value is one order of magnitude higher than the value obtained in this study. Haffener (2017) uses a median value of 0.5 m²/s for simulations of induced seismicity in Oklahoma.

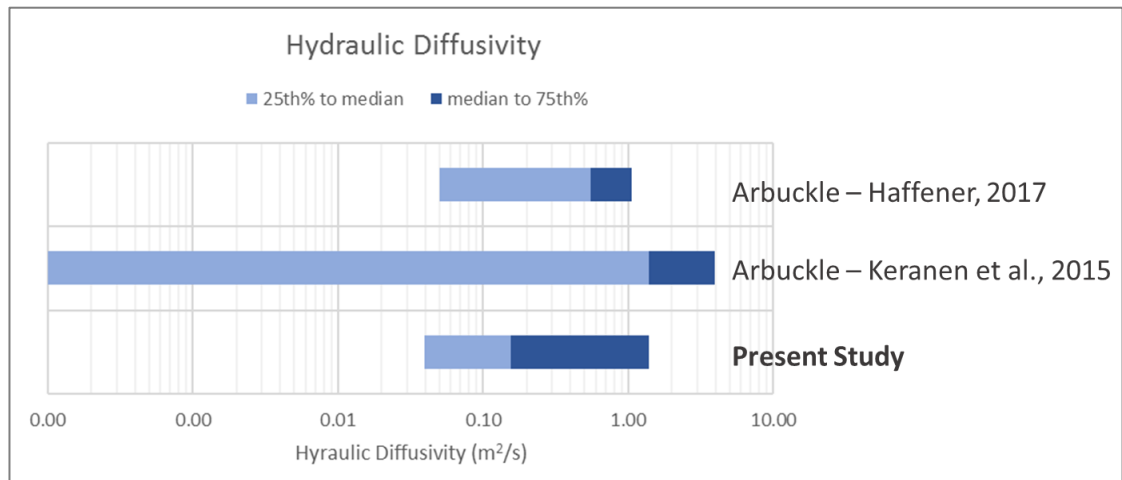


Figure 17. Range of D computed values from solid earth tide analyses (present study) and comparison from previous studies.

Chapter 4: Conclusions

This study shows that fluid levels in the Arbuckle Group in northwestern and north-central Oklahoma respond to solid earth tides (in the six study wells), which is a surrogate of pore pressure in the host rock. Property values of the Arbuckle Simpson Aquifer or the Arbuckle Group, published in the literature or used in modeling studies as input parameters, differ from the values obtained in this study. Most previous studies are representing the Arbuckle Group in combination with the Simpson Group in places where the unit outcrops or in semi-confined portions of the aquifer. Rock properties from the Arbuckle Simpson Aquifer were used as input for hydrogeologic and geomechanical models (Walsh and Zoback, 2015) and simulation of injection scenarios. Using such values for hydrogeologic and geomechanical models results in estimates of extreme and unrealistic pore pressure increases in the Arbuckle Group.

Time-series analyses of the temporal and cyclic patterns of water levels in the wells allowed for estimation of hydraulic and rock properties of the Arbuckle Group in the Anadarko Shelf and the Cherokee Platform geological provinces of Oklahoma. Values obtained for each of the properties computed in this study are consistent with what would be expected for a confined reservoir for the carbonate dominated Arbuckle Group. Table 4 presents the summary of values obtained for elastic and hydraulic properties of the Arbuckle Group from solid earth tides. Using the permeability, porosity, and storage coefficient values obtained in the present study, simulated increases in pore pressure in the Arbuckle Group would be much lower than hypothesized in previous studies.

Table 4. Summary of values obtained for each property computed from solid earth tides time series analyses.

| Well | Tidal Component | Specific Storage (m-1) | Storage coefficient (dimensionless) | Transmissivity (m ² /d) | Barometric Efficiency (dimensionless) | Porosity (percentage) | Matrix Compressibility (psi-1) | Hydraulic Conductivity (m/s) | Intrinsic Permeability (mD) | Hydraulic Diffusivity (m ² /s) |
|------------|-----------------|------------------------|-------------------------------------|------------------------------------|---------------------------------------|-----------------------|--------------------------------|------------------------------|-----------------------------|---|
| Alfalfa 03 | O1 | 1.50E-06 | 1.13E-03 | 12.07 | 0.42 | 16% | 6.18E-07 | 1.87E-07 | 29.03 | 3.87 |
| | M2 | 6.11E-07 | 4.60E-04 | 6.72 | | 7% | 2.52E-07 | 1.04E-07 | 16.16 | 4.91 |
| Alfalfa 04 | O1 | 2.66E-06 | 8.18E-04 | 3.75 | 0.74 | 52% | 4.94E-07 | 1.42E-07 | 22.08 | 0.05 |
| | M2 | 2.00E-06 | 6.14E-04 | 2.09 | | 39% | 3.71E-07 | 7.90E-08 | 12.29 | 0.04 |
| Grant 06 | O1 | 2.34E-06 | 1.05E-03 | 375.48 | 0.87 | 54% | 2.21E-07 | 9.78E-06 | 1520.89 | 4.17 |
| | M2 | 1.28E-06 | 5.71E-04 | 194.11 | | 29% | 1.20E-07 | 5.05E-06 | 786.23 | 3.95 |
| Lincoln 10 | O1 | 2.20E-06 | 2.57E-03 | 18.77 | 0.68 | 39% | 5.03E-07 | 1.87E-07 | 29.06 | 0.08 |
| | M2 | 8.93E-07 | 1.04E-03 | 13.44 | | 16% | 2.04E-07 | 1.34E-07 | 20.8 | 0.15 |
| Pawnee 11 | O1 | 1.28E-06 | 2.14E-04 | 14.44 | 0.61 | 21% | 3.51E-07 | 1.00E-06 | 155.84 | 0.78 |
| | M2 | 3.38E-07 | 5.67E-05 | 8.20 | | 5% | 9.26E-08 | 5.69E-07 | 88.43 | 1.68 |
| Logan 12 | O1 | 1.80E-06 | 6.74E-04 | 14.72 | 0.54 | 26% | 5.83E-07 | 4.58E-07 | 71.26 | 0.25 |
| | M2 | 4.30E-07 | 1.61E-04 | 8.20 | | 7% | 1.39E-07 | 2.55E-07 | 39.67 | 0.59 |
| | Median | 1.39E-06 | 6.44E-04 | 12.76 | 0.65 | 24% | 3.02E-07 | 2.21E-07 | 34.37 | 0.69 |

References

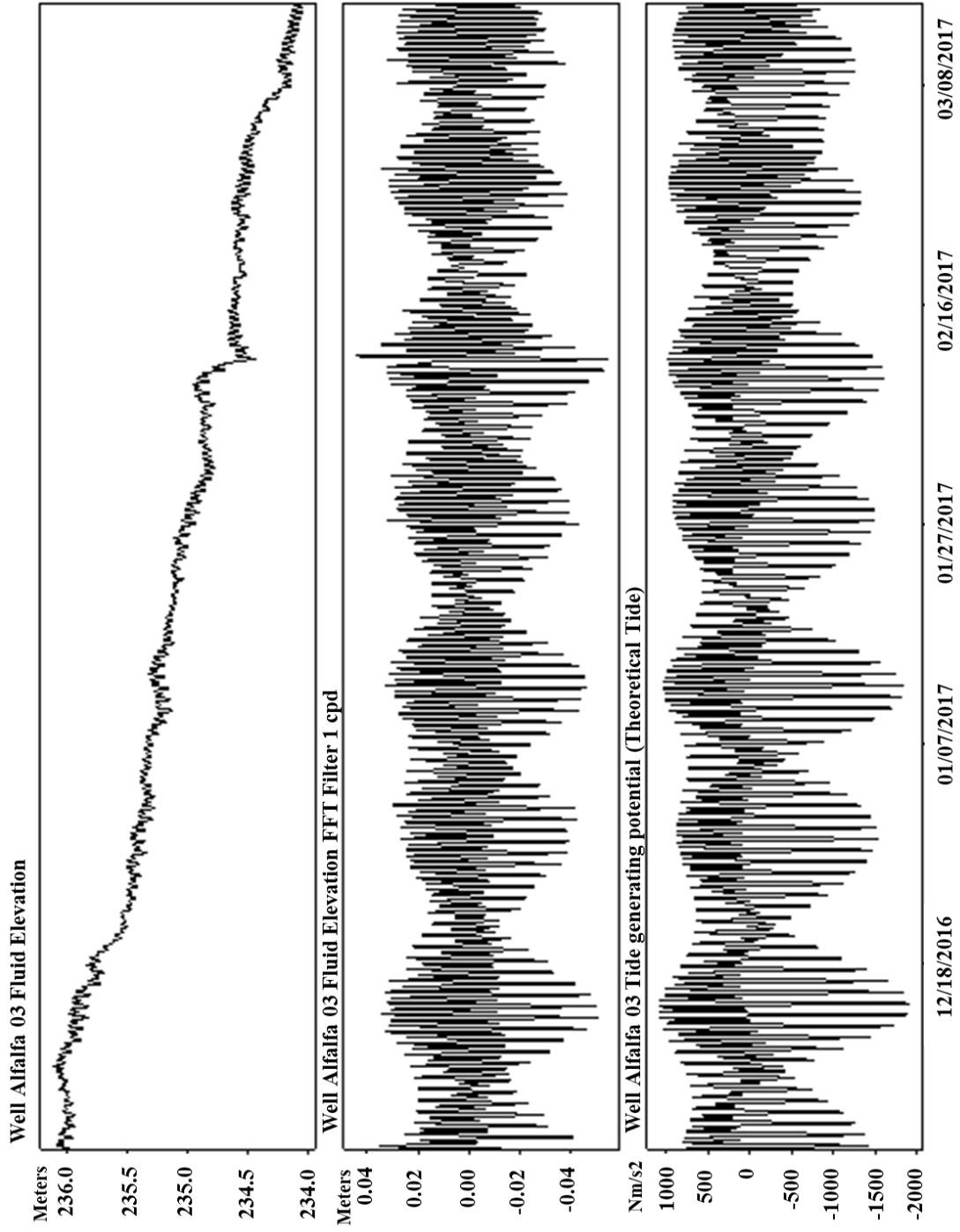
- Acworth, R. I., Rau, G. C., McCallum, A. M., Andersen, M. S., and Cuthbert, M. O., 2015, Understanding connected surface-water/groundwater systems using Fourier analysis of daily and sub-daily head fluctuations: *Hydrogeology Journal*, v. 23, p. 17.
- Bernard, S., and Delay, F., 2008, Determination of porosity and storage capacity of a calcareous aquifer (France) by correlation and spectral analyses of time series: *Hydrogeology Journal*, v. 16, p. 11.
- Bredehoeft, J. D., 1967, Response of Well-Aquifer Systems to Earth Tides: *Journal of Geophysical Research: Solid Earth*, v. 72, no. 12, p. 13.
- Carr, J. E., McGovern, H. E., Gogel, T., and Doveton, J., 1986, Geohydrology of and Potential for Fluid Disposal in the Arbuckle Aquifer in Kansas with a section on Log Analysis of the Arbuckle Aquifer: U.S.G.S. Geological Survey, v. Open-file Report 86-491, p. 109.
- Carrell, J., 2014, Field-Scale Hydrogeologic Modeling of Water Injection into the Arbuckle Zone of the Midcontinent, p. 101.
- Christenson, S., Hunt, A. G., and Parkhurst, D. L., 2009, Geochemical Investigation of the Arbuckle-Simpson Aquifer, South-Central Oklahoma, 2004-06: US Geological Survey Scientific Investigations Report, v. 2009-5036, p. 60.
- Christenson, S., Osborn, N. I., Neel, C. R., Faith, J. R., Bloom, C. D., Puckette, J., and Pantea, M. P., 2011, Hydrogeology and Simulation of Groundwater Flow in the Arbuckle-Simpson Aquifer, South-Central Oklahoma: U.S.G.S. Geological Survey, v. Scientific Investigations Report 2011-5029, p. 121.
- Cuttillo, P. A., and Bredehoeft, J. D., 2011, Estimating Aquifer Properties from the Water Level Response to Earth Tides: *Groundwater*, v. 49, no. 4, p. 11.
- Doodson, A. T., and Warburg, H. D., 1941, Admiralty manual of tides: Her Majesty's Stationary Office.
- Fetter, C. W., 2013, *Applied Hydrogeology*, United Kingdom, Always learning, 612 p.:
- Freeze, R. A., and Cherry, J. A., 1979, *Groundwater*, Englewood Cliffs, NJ.
- Fritz, R. D., Medlock, P., Kuykendall, M. J., and Wilson, J. L., 2013, The Geology of the Arbuckle Group in the Midcontinent: Sequence Stratigraphy, Reservoir Development, and the Potential for Hydrocarbon Exploration: *AAPG Memoir*, v. 98, p. 72.

- Hsieh, P. A., Bredehoeft, J. D., and Farr, J. M., 1987, Determination of aquifer transmissivity from earth tide analysis: *Water Resources Research*, v. 23, no. 10, p. 8.
- Johnson, K. S., 1991, *Geologic Setting of the Arbuckle Group in Oklahoma: Oklahoma Geological Survey Special Publication*, v. 91-3, p. 5.
- , 2008, *Geologic History of Oklahoma: Oklahoma Geological Survey Educational Publication*, v. 9, p. 6.
- Keranen, K. M., Savage, H. M., Abers, G. A., and Cochran, E. S., 2013, Potentially induced earthquakes in Oklahoma, USA: Links between wastewater injection and the 2011 Mw 5.7 earthquake sequence: *Geology*, v. 41, no. 6, p. 4.
- Keranen, K. M., Weingarten, M., Albers, G. A., Bekins, B. A., and Ge, S., 2014, Sharp increase in central Oklahoma seismicity since 2008 induced by massive wastewater injection: *Science*, v. 345, no. 6195, p. 5.
- Kroll, K. A., Cochran, E. S., and Murray, K. E., 2017, Poroelastic properties of the Arbuckle Group in Oklahoma derived from well fluid level response to the 3 September 2016 Mw5.8 Pawnee and 7 November 2016 Mw5.0 Cushing Earthquakes: *Seismological Research Letters*, v. In press, p. 22.
- Maréchal, J. C., Sarma, M. P., Ahmed, S., and Lachassagne, P., 2002, Establishment of earth tides effect on water level fluctuations in an unconfined hard rock aquifer using spectral analysis: *Current Science, Indian Academy of Sciences*, v. 83, no. (1), p. 12.
- Marsaud, B., Mangin, A., and Bel, F., 1993, Estimation des caractéristiques physiques d'acuífères profonds à partir de l'incidence barométrique et des marées terrestres: *Journal of Hydrology*, v. 144, p. 16.
- Mehnert, E., Valocchi, A. J., Heidari, M., Kapoor, S. G., and Kumar, P., 1999, Estimating Transmissivity from the Water Level Fluctuations of a Sinusoidal Forced Well: *Groundwater*, v. 37, no. 6, p. 6.
- Merritt, M. L., 2004, *Estimating Hydraulic Properties of the Floridian Aquifer System by Analysis of Earth-tide, Ocean-Tide, and Barometric Effects, Collier and Hendry Counties, Florida: US Geological Survey Water-Resources Investigations Report*, v. 03-4267, p. 76.
- Morgan, B. C., and Murray, K. E., 2015, *Characterizing Small-Scale Permeability of the Arbuckle Group, Oklahoma: Oklahoma Geological Survey Open-File Report*, v. OF2-2015, p. 16.

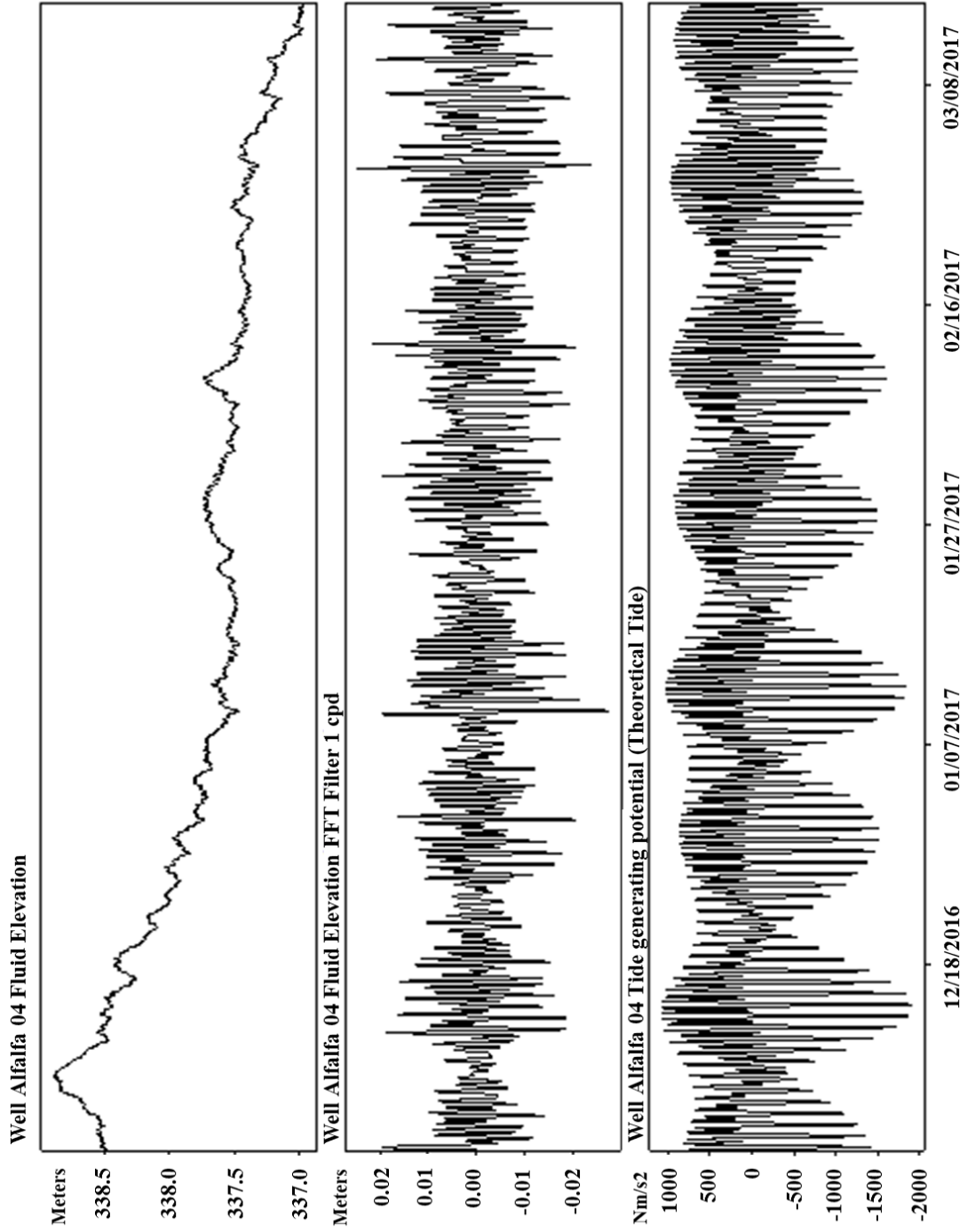
- Munk, W. H., and MacDonald, G. J. F., 1960, *The Rotation of the Earth: A Geophysical Discussion*: Cambridge University Press.
- Murray, K. E., 2015, *Class II Saltwater Disposal for 2009-2014 at the Annual-, State-, and County- Scales by Geologic Zones of Completion, Oklahoma*: Oklahoma Geological Survey Open-File Report, v. OF5-2015, p. 22.
- Murray, K. E., and Holland, A., 2014, *Inventory of Class II Underground Injection Control Volumes in the Midcontinent: Shale Shaker*, v. March-April 2014, p. 9.
- Northcutt, R. A., and Campbell, J. A., 1995, *Geological provinces of Oklahoma*: Oklahoma Geological Survey Open-File Report, v. OF5-95.
- Ragland, D. A., and Donovan, R. N., 1991, *Sedimentology and Diagenesis of the Arbuckle Group in Outcrops of Southern Oklahoma*: Oklahoma Geological Survey Special Publication, v. 91-3, p. 21.
- Rahi, K. A., 2010, *Estimating the hydraulic parameters of the Arbuckle-Simpson Aquifer by analysis of naturally-induced stresses: Doctoral Dissertation* Oklahoma State University, p. 168.
- Todd, D. K., 1980, *Groundwater Hydrology*, New York 535 p.:
- Van-Camp, M., and Vauterin, P., 2005, *Tsoft: graphical and interactive software for the analysis of time series and Earth tides*: *Computers & Geosciences*, v. 31, p. 10.
- Walsh, F. R., and Zoback, M. D., 2015, *Oklahoma's recent earthquakes and saltwater disposal*: *Science Advances*, v. 1, p. 9.
- Weingarten, M., 2015, *On the interaction between fluids and earthquakes in both natural and induced seismicity*, p. 207.
- Weingarten, M., Ge, S., Godt, J. W., Bekins, B. A., and Rubinstein, J. L., 2015, *High-rate injection is associated with the increase in U.S. mid-continent seismicity*: *Science*, v. 348, no. 6241, p. 6.
- Witze, A., 2015, *Artificial quakes shake Oklahoma*: *Nature*, v. 520, p. 2.

Appendix A: Monitoring Wells Observed Solid Earth Tides

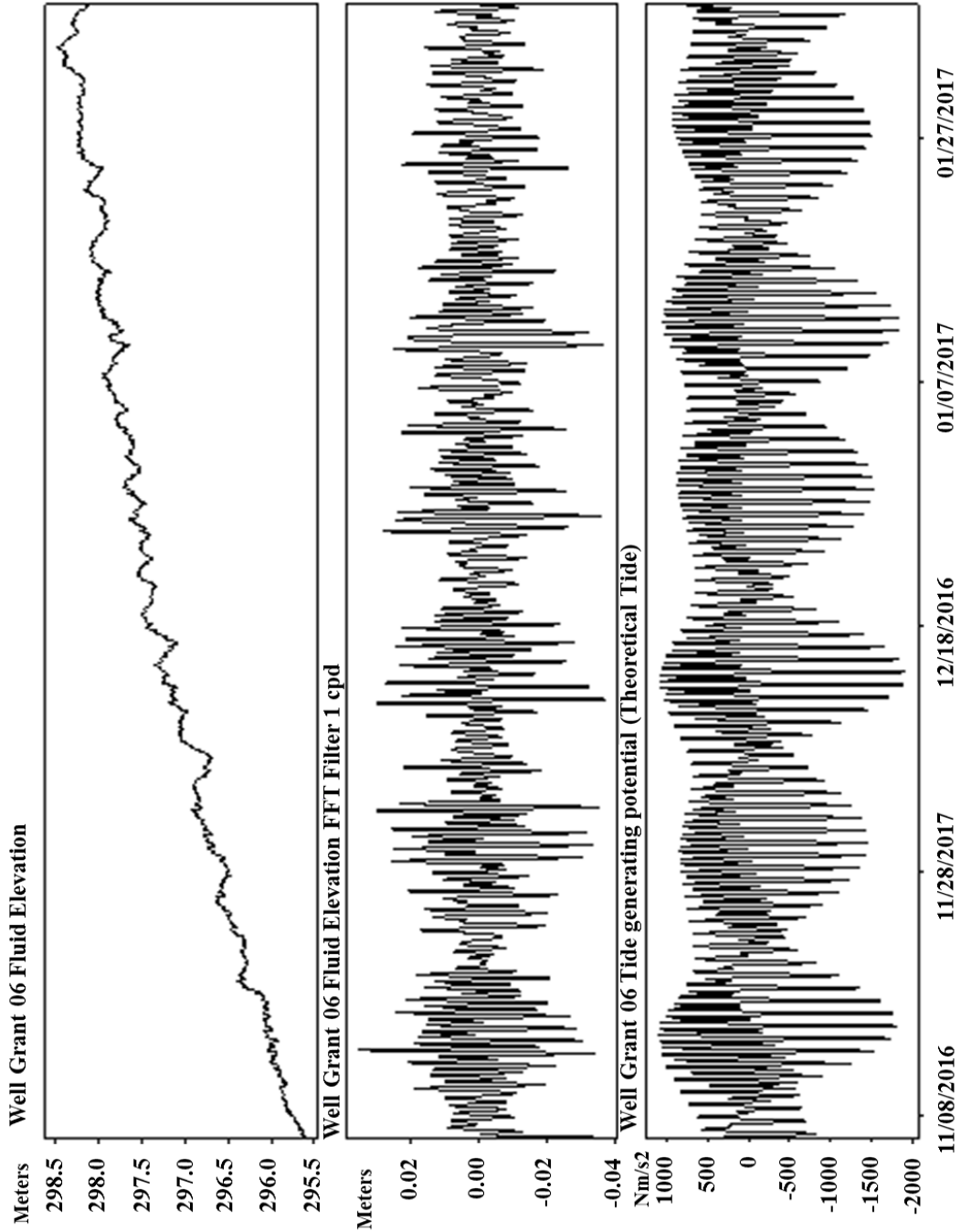
A-1 Well Alfalfa 03



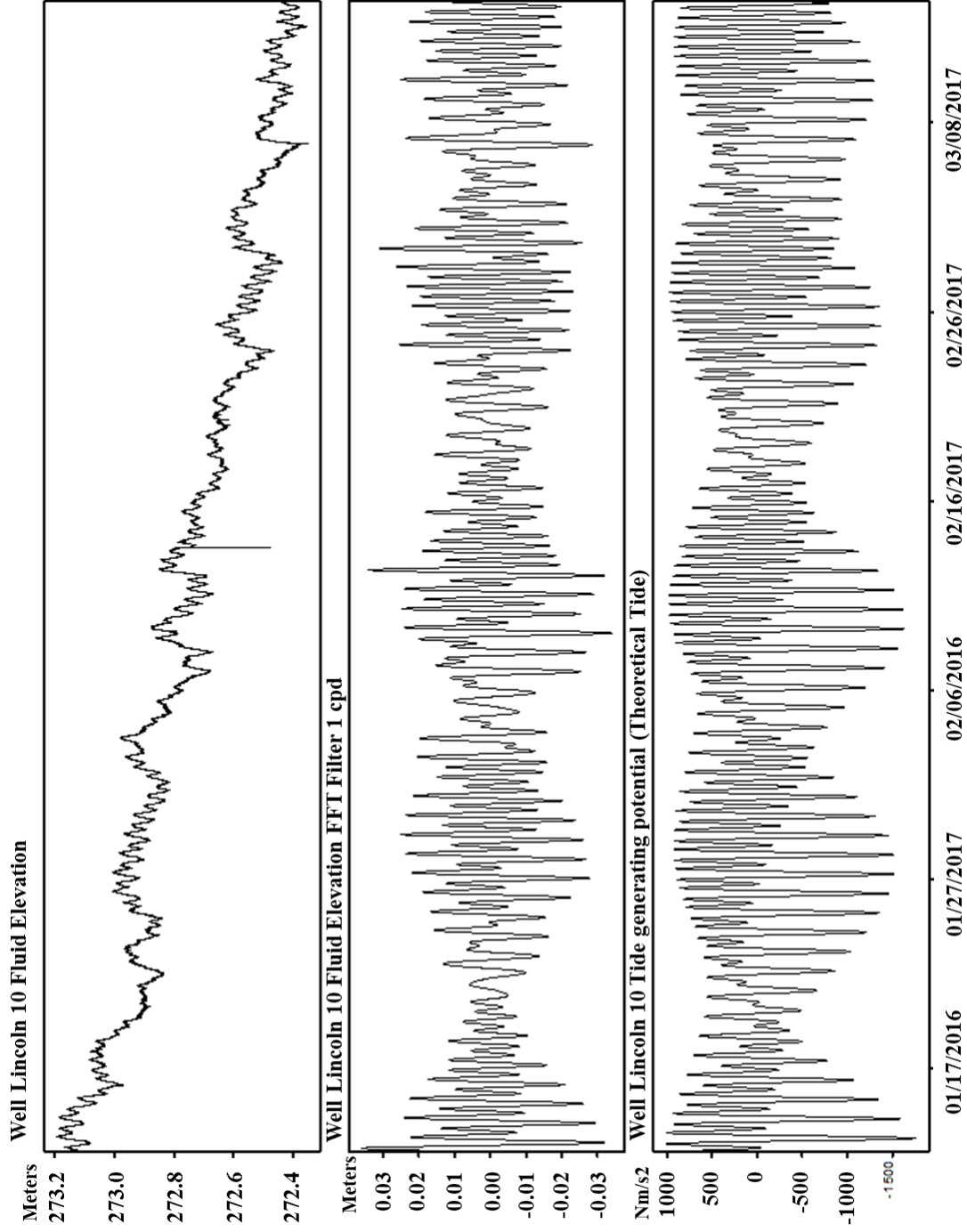
A-2 Well Alfalfa 04



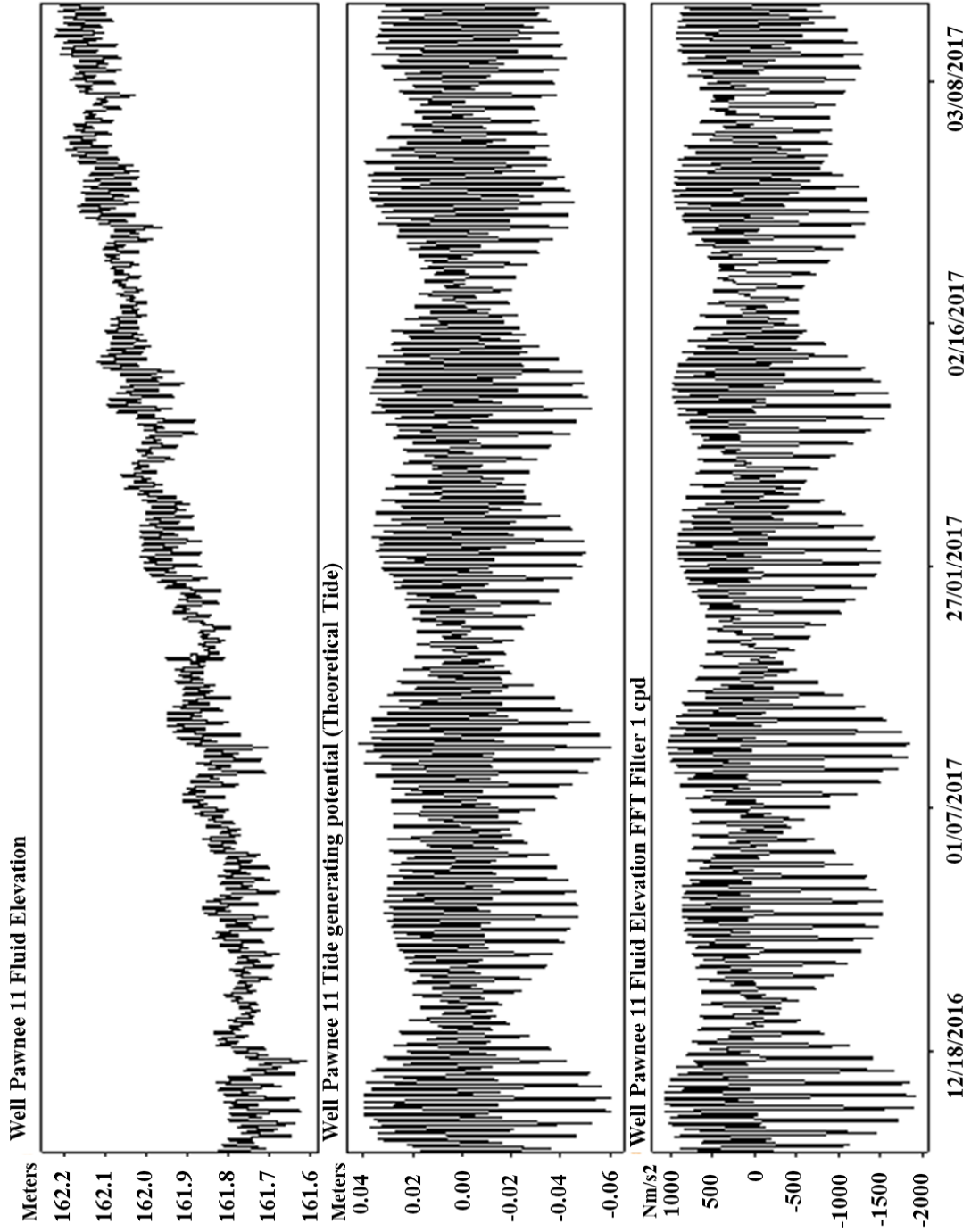
A-3 Well Grant 06



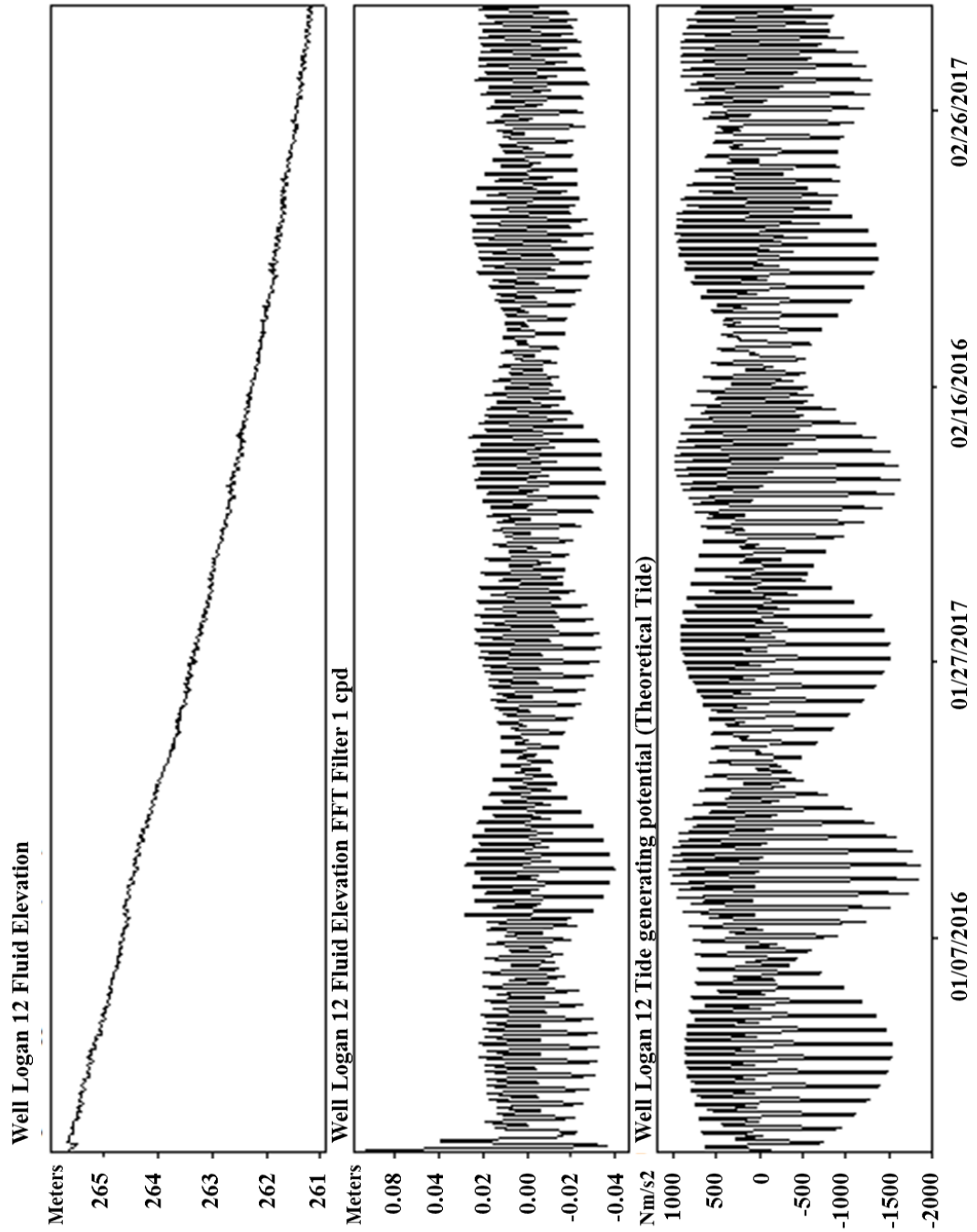
A-4 Well Lincoln 10



A-5 Well Pawnee 11

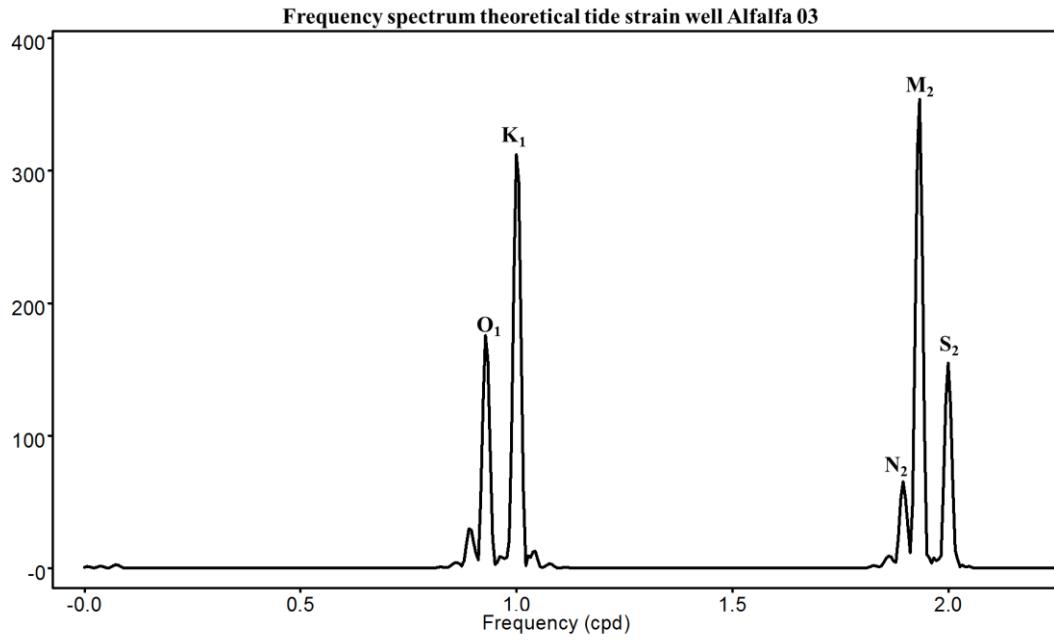
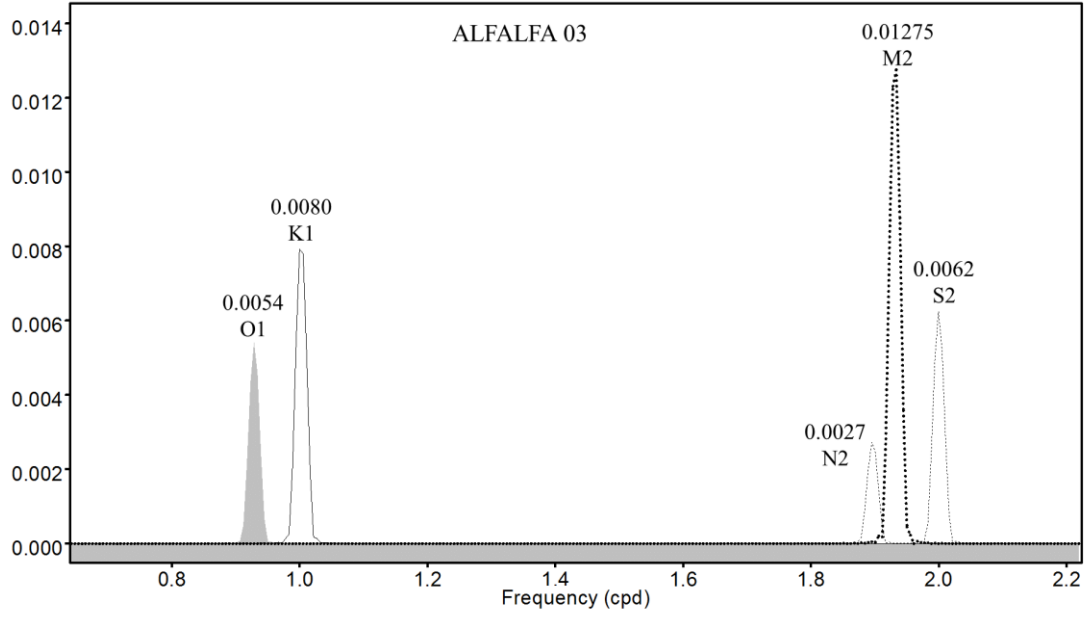


A-6 Well Logan 12

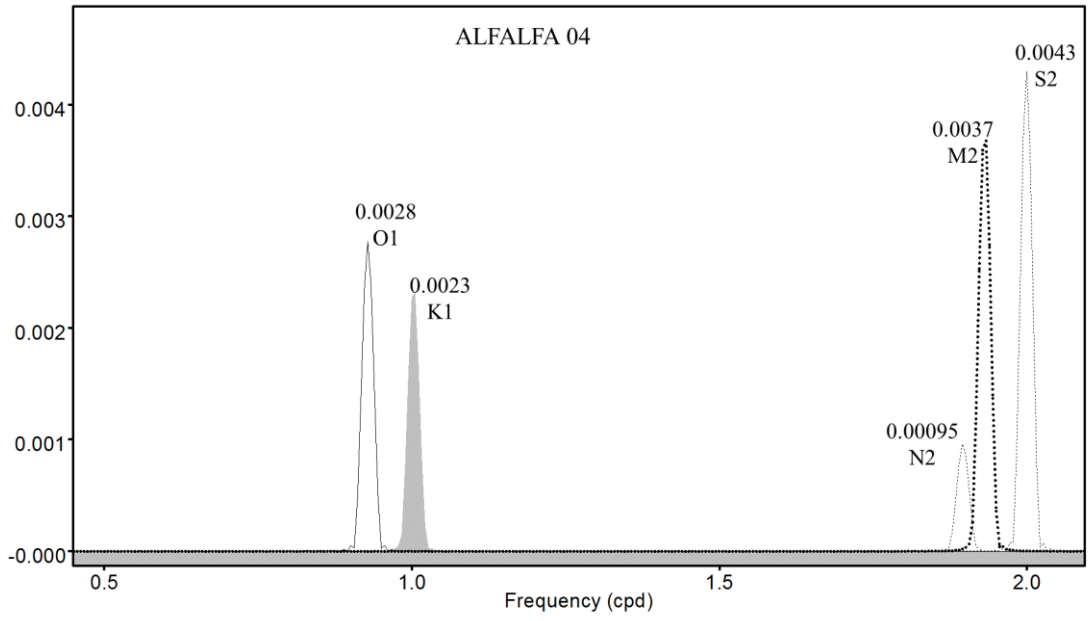


**Appendix B: Frequency Spectrum For Monitoring Wells And
Theoretical Solid Earth Tides**

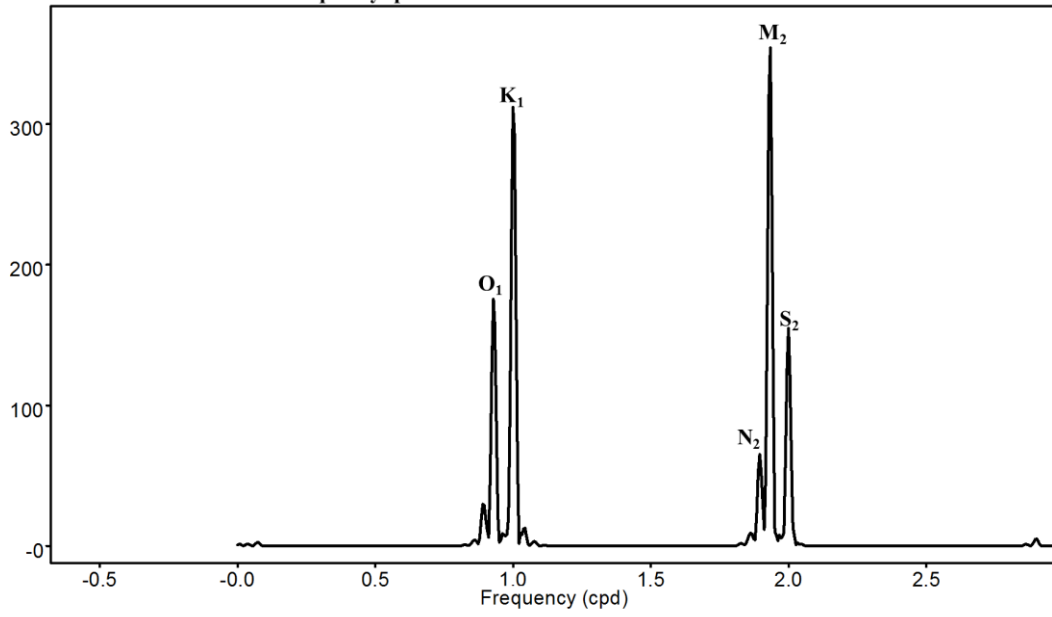
B-1 Well Alfalfa 03



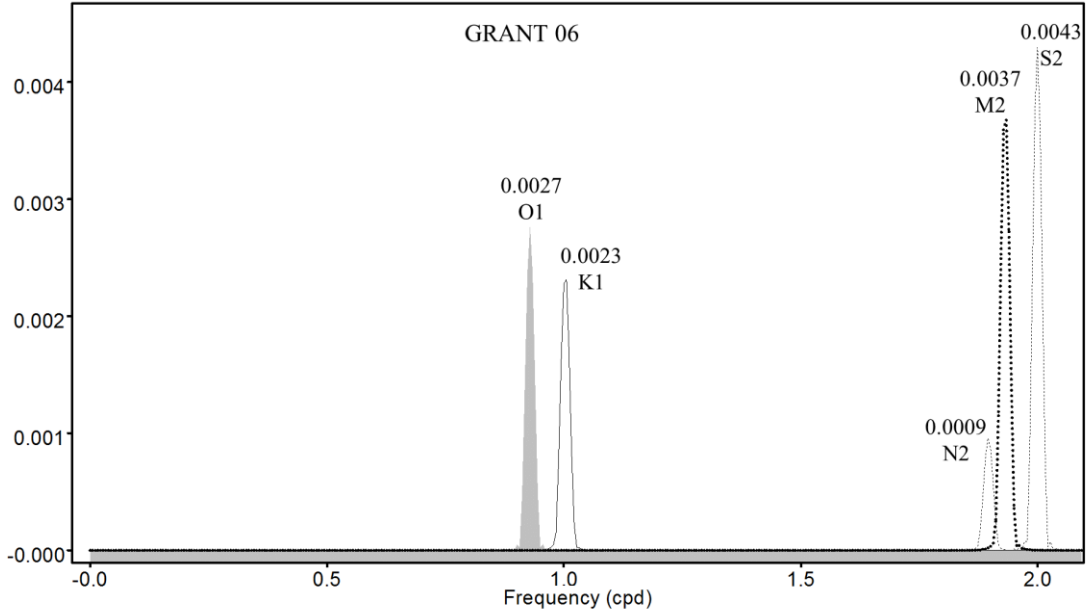
B-2 Well Alfalfa 04



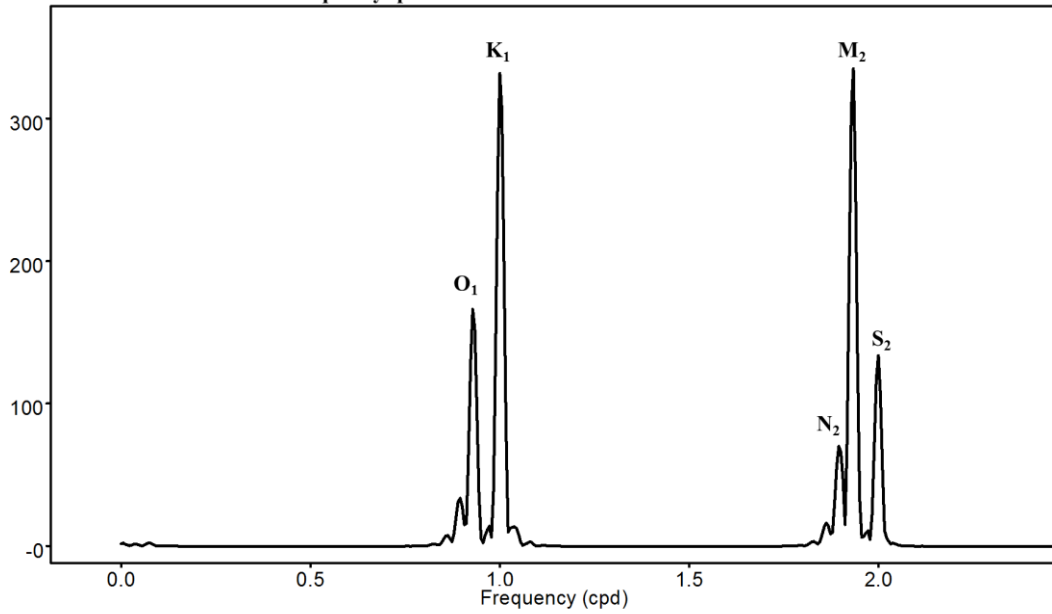
Frequency spectrum theoretical tide strain well Alfalfa 04



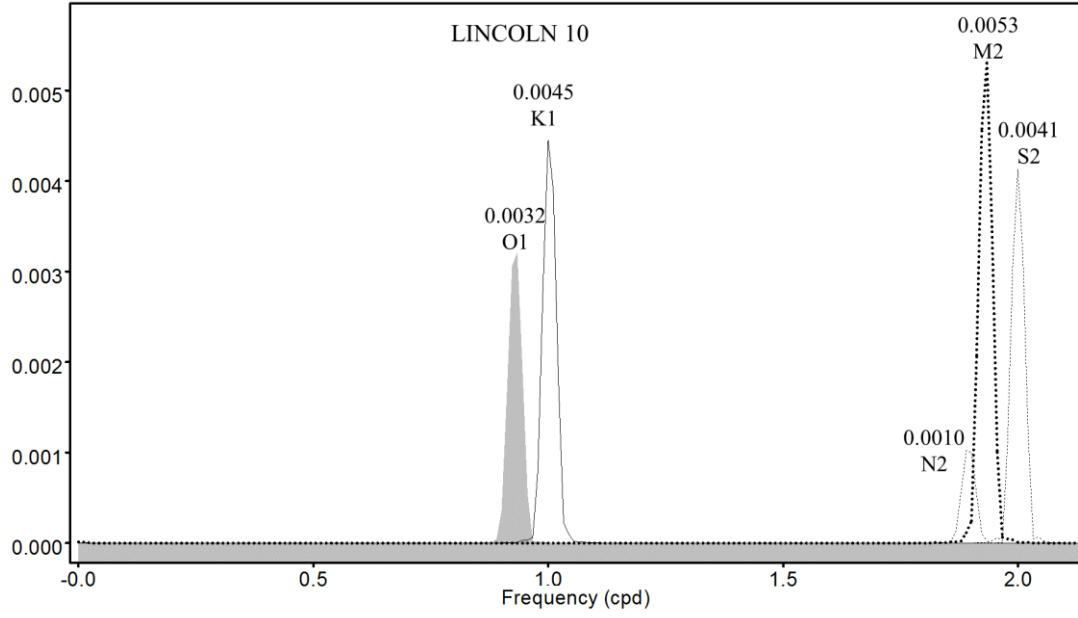
B-3 Well Grant 06



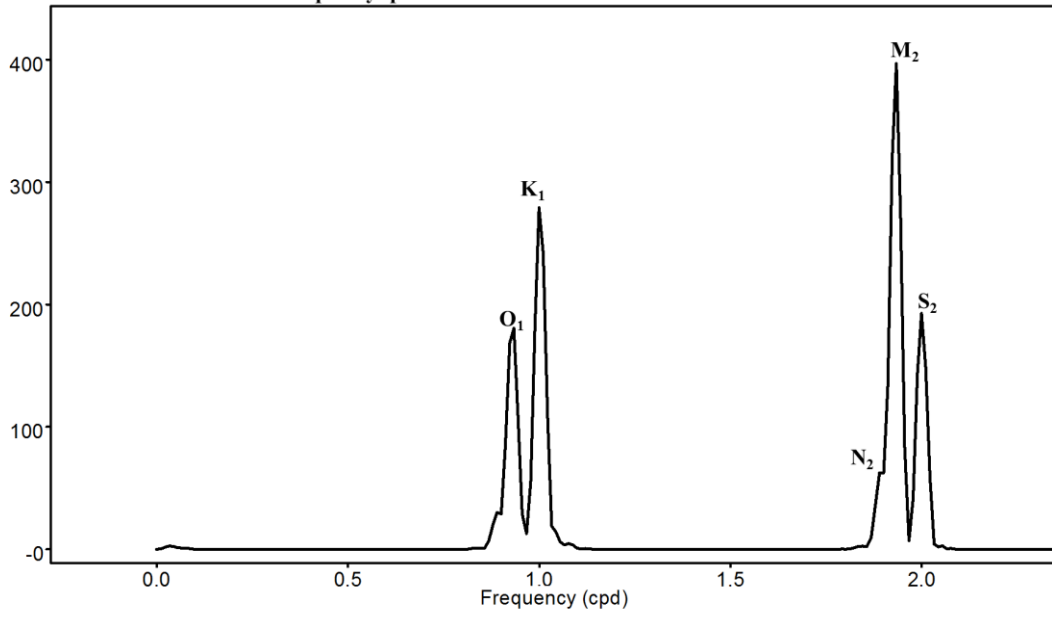
Frequency spectrum theoretical tide strain well Grant 06



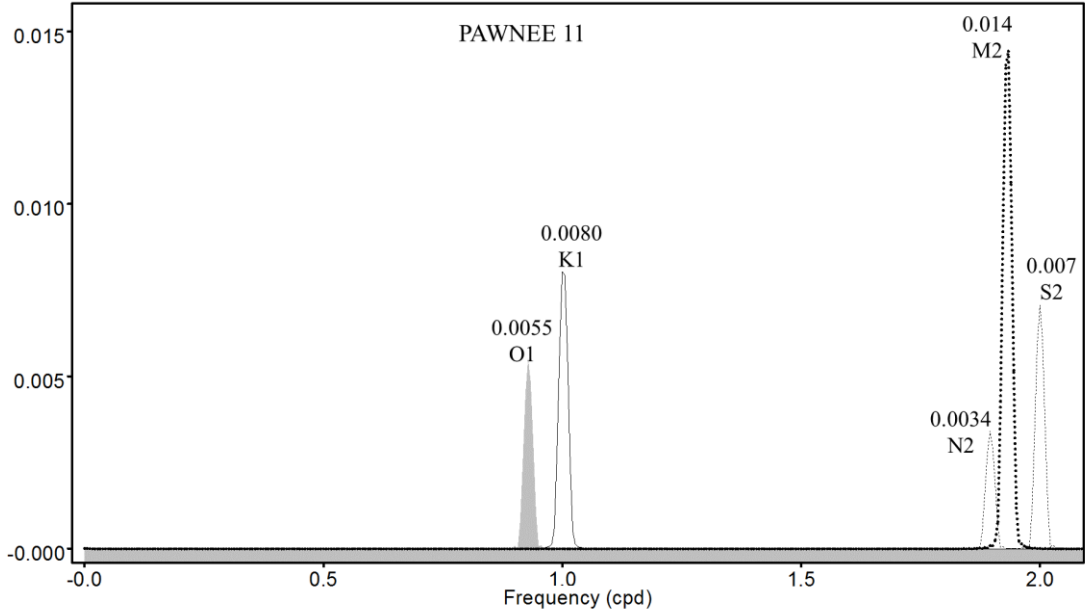
B-4 Well Lincoln 10



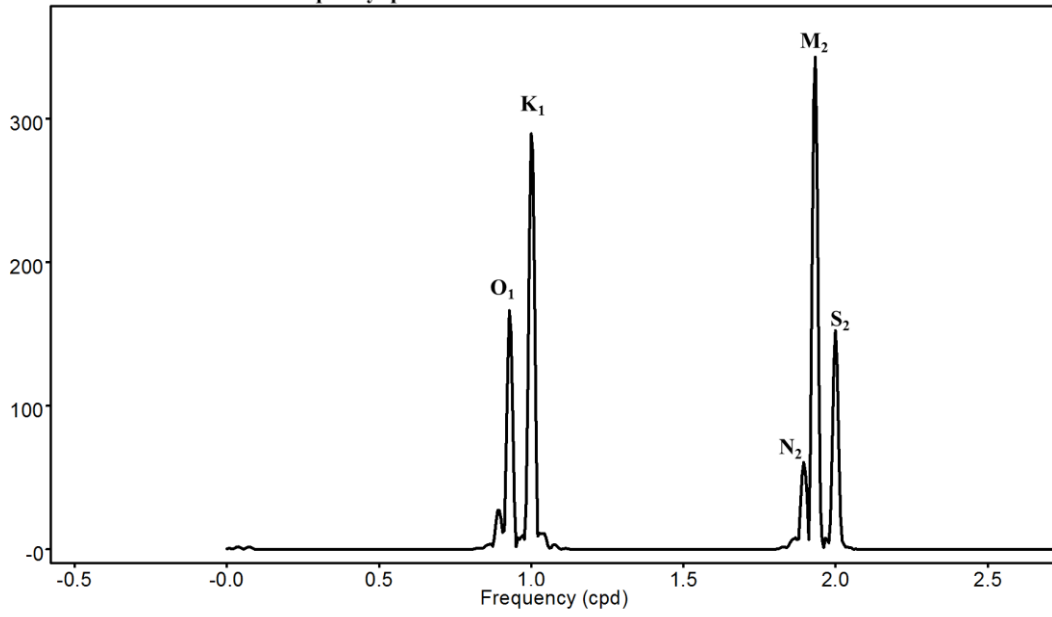
Frequency spectrum theoretical tide strain well Lincoln 10



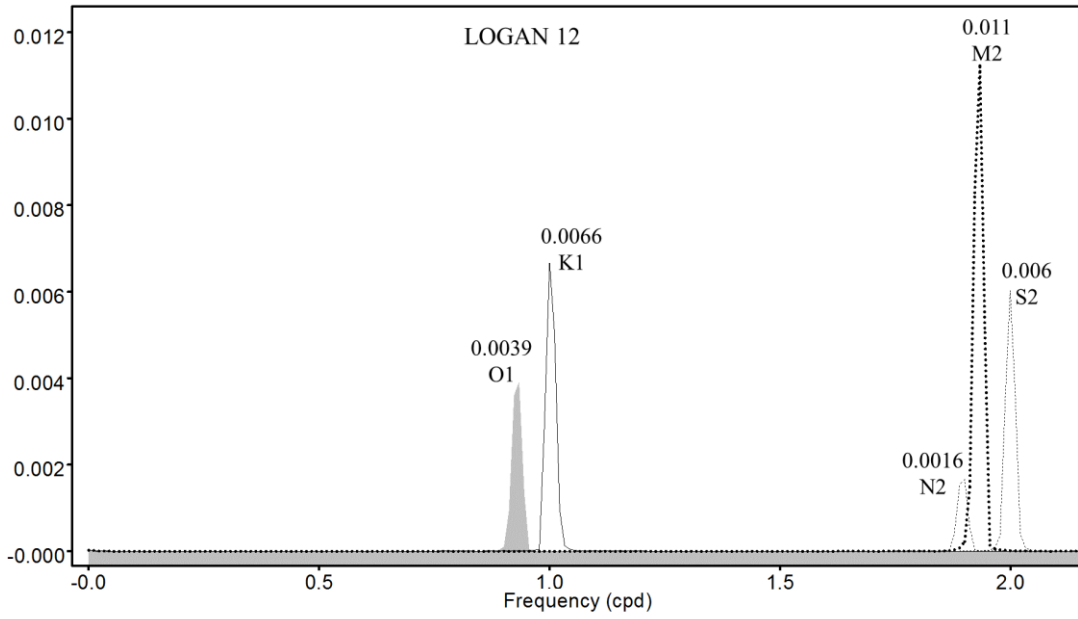
B-5 Well Pawnee 11



Frequency spectrum theoretical tide strain well Pawnee 11



B-6 Well Logan 12



Frequency spectrum theoretical tide strain well Logan 12

